

β -Arrestin-mediated Regulation of the Human Ether-a-go-go-Related Gene (hERG) Potassium
Channel

by

Matthew Sangoi

A thesis submitted to the Graduate Program in Experimental Medicine

Department of Biomedical and Molecular Sciences

In conformity with the requirements for
the degree of Master of Science

Queen's University

Kingston, Ontario, Canada

(August, 2016)

Copyright ©Matthew Sangoi, 2016

Abstract

The *human ether-a-go-go-related gene (hERG)* encodes the voltage-gated K⁺ channel, hERG (Kv11.1). This channel passes the rapidly-activating delayed rectifier K⁺ current (I_{Kr}), which is important for cardiac repolarization. A reduction in I_{Kr} due to loss-of-function mutations or drug interactions causes long QT syndrome (LQTS), which can lead to cardiac arrhythmias and sudden cardiac death. The density of hERG channels in the plasma membrane is a key determinant of normal physiological function, and is balanced by trafficking to and from the cell surface. Many LQTS-associated hERG mutations result in a trafficking deficiency of otherwise functional channels. Thus, elucidating mechanisms of hERG regulation at the plasma membrane is useful for the prevention and treatment of LQTS. We previously demonstrated that M3 muscarinic receptor activation increases mature hERG expression through a G_q protein-dependent protein kinase C (PKC) pathway. In addition to conventional G_q protein-coupling, M3 receptors recruit β-arrestins upon agonist binding. Traditionally known for their role in receptor desensitization and internalization, β-arrestins also act as adaptor proteins to facilitate G protein-independent signaling. In the present work, I investigated the exclusive effect of β-arrestin signaling on hERG expression by utilizing an arrestin-biased M3 designer receptor (M3D-arr) exclusively activated by clozapine-*N*-oxide (CNO). By expressing M3D-arr in hERG-HEK cells and treating with CNO under various conditions, I found that M3D-arr activation increased mature hERG expression and current. Within this paradigm, M3D-arr recruited β-arrestin to the plasma membrane, and promoted the PI3K-dependent activation of Akt. I further found that the activated Akt acted through phosphatidylinositol 3-phosphate 5-kinase (PIKfyve) and Rab11 to facilitate endosomal recycling of hERG channels to the plasma membrane.

Co-Authorship

Shawn Lamothe assisted in the experimental design, acquisition of Western blot, co-immunoprecipitation, and immunocytochemistry data. Jun Guo and Wentao Li performed patch-clamp experiments and data acquisition. Tonghua Yang assisted in the preparation of immunocytochemistry experiments and procurement of immunofluorescent confocal images.

Acknowledgements

After completing my undergraduate degree in Life Science at Queen's University, during which I conducted an undergraduate thesis project, I knew that I wanted to pursue research at the graduate level. Although entering the Experimental Medicine program with some experience, I knew there would be much for me to learn over the next two years. As I near the end of my MSc. degree, I realize how much I have learned as a researcher and as a person. The knowledge and skills I have acquired in the Zhang lab will undoubtedly prepare me for what lies ahead. My achievements throughout the program can be attributed to hard work, dedication, and perseverance; however, none of it would be possible without the help and support of many individuals in my life.

First and foremost, I would like to thank my family. From my undergraduate to graduate studies, their multifaceted support has helped me every step of the way. As the first person in my family to attend university, they ensured I overcame any obstacle that life or school presented. I would like to thank my brother, Chris, who consistently reinforced my confidence as a student, and helped me get through many stressful times. I would also like to thank my mother, who has shaped me into the person I am today. Her constant emotional and financial support has allowed me to succeed in all of my educational endeavors. The focus, dedication, hard work she installs into her life and career have been a true inspiration to me, and are reflected in my university studies. Thank you both for all your support. I could not have accomplished anything without you.

Second, I would like to thank all of my friends, whom I have met over the past two years and those whom I have known for many years. All of my friends have provided me with endless encouragement during my time at Queen's University, helping me maintain my enthusiasm and

motivation in school. In particular, I would like to thank the Boyz from back home. We have known each other for a very long time, and our support for one another is unrivaled. My more recent friends, who share the same goals and interests in medical research, have not only strengthened my understanding in the field, but have driven me to conduct the highest quality research.

Thirdly, I would like to thank all the members of the Zhang lab who I have interacted with on a daily basis. The encouraging attitude and selfless actions of every individual makes the lab very efficient, but also an enjoyable place to conduct research. Thank you to Shawn Lamothe, who has been the biggest influence in the development of my project on the M3 DREADD receptor. I appreciate the countless hours he put toward helping me design and execute experiments. He assisted in my training on cell culture techniques, co-immunoprecipitations, and immunofluorescence microscopy, and performed many patch clamp experiments for my project. Thank you to John Szendrey, for not only helping me get into the lab, but for all the training when I first started two years ago. We've been through a lot of school together, but it was nice to have a familiar face in the lab while getting adjusted. Thank you to Jun Guo, who is a foundational member of the lab, providing everyone with high quality cells, conducting patch clamp experiments, and analyzing copious amounts of data. His professional and kind attitude provided me with comfort, knowing he would be willing to help with any experiment. Thank you to Tonghua for assisting with immunocytochemistry and RT-qPCR experiments. Your willingness to help acquire perfect data sets had a tremendous impact on the quality of my work. Thank you to Wentao Li, for maintaining the lab to such a high standard, and for performing countless patch clamp experiments. I would also like to thank my fellow graduate students, Yudi Kang, Andrew Hogan-Cann, Ellen Avery, and Gianni Sampieri, who

have made the lab an enjoyable place to work each and every day. And to the undergraduate students in the lab, Jordan Davis and Aja Hogan-Cann, your high level of enthusiasm and positive attitude always brighten the lab environment.

Last but not least, I would like to thank Dr. Shetuan Zhang. You are one of the hardest working, dedicated, and motivated researchers I have met. Such qualities have definitely shaped and influenced my work ethic over the past two years, as I am sure they will for future students to come. Your inherent drive to motivate students and passion for quality research has had a profound impact on my graduate experience. As a supervisor, your ability to maintain such a successful lab and deeply engage in every student's project is highly praised.

Table of Contents

Abstract	ii
Co-Authorship.....	iii
Acknowledgements.....	iv
List of Figures	ix
List of Abbreviations	x
Chapter 1 : Introduction and Literature Review	1
1.1 Cardiac Repolarization and Long QT Syndrome.....	1
1.2 The hERG K ⁺ Channel	4
1.2.1 Structure	4
1.2.2 Kinetics and Gating	6
1.2.3 Biosynthesis and Trafficking	8
1.2.4 Internalization and Degradation	9
1.3 Rab GTPases	10
1.4 Phosphoinositide-3 kinase (PI3K) Signaling	14
1.4.1 PI3K-dependent Activation of Akt	16
1.4.2 PI3K/Akt Signaling in Cardiac Electrophysiology.....	17
1.5 β -arrestins	18
1.5.1 Traditional GPCR Signaling	18
1.5.2 β -arrestin-dependent Signaling	19
1.6 Designer Receptors Exclusively Activated by Designer Drugs (DREADDs).....	21
Hypothesis and Objectives	24
Chapter 2 : Materials and Methods.....	26
2.1 Molecular Biology.....	26
2.2 Western Blot Analysis.....	27
2.3 Co-immunoprecipitation	28
2.4 RNA Extraction and Quantitative Reverse Transcription.....	28
2.5 Immunofluorescence Microscopy	29
2.6 Patch Clamp Recording.....	29
2.7 Reagents and Antibodies.....	30

2.8 Statistical Analysis	30
Chapter 3 : Results	31
3.1 CNO-mediated activation of M3D-arr increases hERG channel expression and current...	31
3.2 CNO enhances the M3D-arr- β -arrestin interaction and co-localization at the plasma membrane.....	36
3.3 CNO-mediated activation of M3D-arr increases hERG expression through an Akt-dependent pathway.....	38
3.4 Inhibition of PIKfyve or Rab11 abolishes the effect of CNO-mediated M3D-arr activation on I_{hERG}	45
Chapter 4 : Discussion	48
Future Directions.....	55
References.....	56

List of Figures

<i>Figure 1. The unique biophysical properties of I_{Ks}, I_{Kr}, and I_{K1} are perfectly adapted to constitute a repolarization reserve.</i>	2
<i>Figure 2. Schematics of hERG channel structure.</i>	5
<i>Figure 3. Gating kinetics of hERG channels.</i>	7
<i>Figure 4. Rab compartmentalization and Rab domains within endosomes.</i>	12
<i>Figure 5. Structure of arrestin-biased M3 designer receptor (M3D-arr).</i>	22
<i>Figure 6. CNO increases mature hERG expression levels in a concentration- and time-dependent manner through M3D-arr activation.</i>	32
<i>Figure 7. CNO-mediated activation of M3D-arr increases mature hERG expression levels without enhancing hERG mRNA expression.</i>	34
<i>Figure 8. CNO-mediated activation of M3D-arr increases I_{hERG}.</i>	35
<i>Figure 9. CNO-mediated M3D-arr activation enhances the β-arrestin-M3D-arr interaction. ...</i>	37
<i>Figure 10. CNO-mediated M3D-arr activation enhances the β-arrestin-1-M3D-arr interaction at the plasma membrane.</i>	39
<i>Figure 11. CNO-mediated M3D-arr activation increases hERG expression through an Akt-dependent pathway.</i>	41
<i>Figure 12. CNO-mediated M3D-arr activation increases the expression level of hERG as well as phosphorylated Akt (p-Akt).</i>	42
<i>Figure 13. CNO-mediated M3D-arr activation increases mature hERG expression and I_{hERG} through PI3K-mediated activation of Akt.</i>	44
<i>Figure 14. The effect of CNO-mediated M3D-arr activation on I_{hERG} is abolished by inhibition of PIKfyve or Rab11.</i>	47
<i>Figure 15. Illustration of M3D-arr-mediated β-arrestin signaling in hERG regulation.</i>	54

List of Abbreviations

ACh	Acetylcholine
Akt	Protein Kinase B
BSA	Bovine Serum Albumin
Ca ²⁺	Calcium Ion
Cav	Caveolin
CNO	Clozapine- <i>N</i> -Oxide
Cs ⁺	Cesium Ion
DREADD	Designer Receptor Exclusively Activated by Designer Drugs
ECG	Electrocardiography
ECL	Enhanced Chemiluminescent
EDTA	Ethylenediaminetetraacetic Acid
EGTA	Ethyleneglycoltetraacetic Acid
ER	Endoplasmic Reticulum
FBS	Fetal Bovine Serum
GFP	Green Fluorescent Protein
HEK	Human Embryonic Kidney
hERG	human Ether-a-go-go Related Gene
HRP	Horseradish Peroxidase
I _{K1}	Inward Rectifier Current
I _{CaL}	Long-lasting Calcium Current
I _{hERG}	hERG Current

I_{Kr}	Rapidly Activating Delayed Rectifier Potassium Current
I_{Ks}	Slowly Activating Delayed Rectifier Potassium Current
I_{Na}	Sodium Current
K^+	Potassium Ion
LQTS	Long QT Syndrome
M3	Muscarinic M3 Receptor
M3D-arr	Arrestin-biased M3 DREADD
MEM	Minimum Essential Medium
Na^+	Sodium Ion
Nedd4-2	Neural Precursor Cell-expressed Developmentally Downregulated protein 4 Type 2
PBS	Phosphate-Buffered Saline
PI3K	Phosphoinositide 3-Kinase
PDK1	Phosphoinositide-dependent Kinase-1
PIKfyve	Phosphatidylinositol 3-phosphate 5-Kinase
PKA	Protein Kinase A
PKB	Protein Kinase B
PKC	Protein Kinase C
PMSF	Phenylmethanesulfonyl Fluoride
PtdIns	Phosphatidylinositol
PTEN	Phosphatase and tensin homologue deleted on chromosome 10
PVDF	Polyvinylidene Difluoride
Rab	Small GTPase Ras-related protein

RIPA	Radioimmunoprecipitation Assay
SDS-PAGE	Sodium Dodecyl Sulfate Polyacrylamide Gel Electrophoresis
SGK	Serum Glucocorticoid-regulated Kinase
siRNA	small interfering RNA
SQTS	Short QT Syndrome
TBS	Tris-Buffered Saline
Ub	Ubiquitin
WT	Wild Type

Chapter 1: Introduction and Literature Review

1.1 Cardiac Repolarization and Long QT Syndrome

The ventricular action potential (AP) is produced through the coordinated function of ion channels that conduct inward, depolarizing and outward, repolarizing currents in cardiomyocytes. Sequential activation and inactivation of these ion channels shapes the cardiomyocyte AP into five distinct phases (phase 0 – 4). Repolarization (phase 3) occurs in response to K^+ efflux, and is essential for re-establishing the resting membrane potential (Figure 1).

The outward K^+ current contributing to repolarization is conducted by several K^+ channels with unique biophysical properties, but overlapping functions (Grant, 2009). These channels include Kv7.1, hERG, and Kir2.1, which constitute the pore-forming α -subunits that conduct I_{Ks} , I_{Kr} , and I_{K1} , respectively (Sanguinetti & Jurkiewicz, 1990; Töpert *et al.*, 1998). Since Kv7.1 channels are voltage-gated and display slow activation, I_{Ks} increases progressively with depolarization until repolarization develops (Grunnet *et al.*, 2005). hERG channels are also voltage-gated and exist in a closed, open, or inactivated (non-conducting) conformation. Transition between the closed and open conformation is slow, while transition between the open and inactivated conformation is rapid. Sustained depolarization results in slow activation of hERG, followed by rapid inactivation (Ferrer *et al.*, 2006). Once repolarization is initiated, hERG rapidly recovers from inactivation to produce significant repolarization while channels slowly close (Smith *et al.*, 1996). The inward rectifying Kir2.1 channel activates once repolarization ensues (-40 mV), contributing to late repolarization and re-establishing the resting membrane potential (Guo & Lu, 2000). Through coordinated and overlapping activity, these

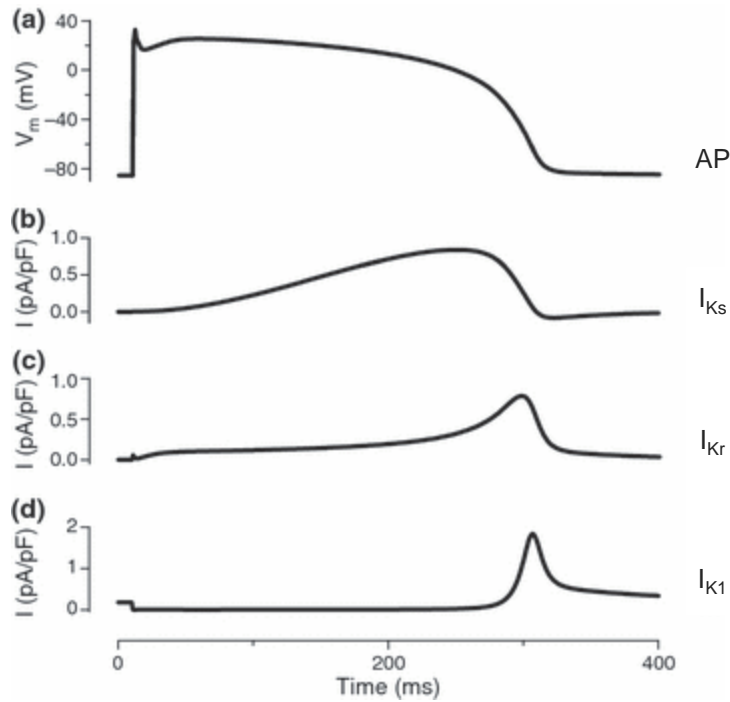


Figure 1. The unique biophysical properties of I_{Ks} , I_{Kr} , and I_{K1} are perfectly adapted to constitute a repolarization reserve.

The coordinated function of I_{Ks} , I_{Kr} , and I_{K1} establish repolarization within cardiomyocytes. (a) A typical ventricular action potential. The current progression for each current is labeled below. (b) The slow activation of I_{Ks} leads to a progressive increase in current during depolarization until repolarization is affected. (c) The initiation of repolarization releases I_{Kr} from inactivation to profoundly impact repolarization, due to the relatively slow deactivation kinetics. (d) Finally, after reaching sufficiently negative membrane potentials, I_{K1} is released from inhibition to contribute to the final part of repolarization and establish the resting membrane potential.

Modified from Grunnet, 2010.

channels effectively generate repolarization, allowing for a subsequent AP to occur. Malfunction of these channels leads to impaired K^+ conductance and reduced repolarization, which can cause arrhythmogenic disease-states such as long QT syndrome.

Long QT syndrome (LQTS) is a cardiac electrical disorder characterized by a prolonged QT interval on an electrocardiogram (ECG) recording. At the cellular level, LQTS is associated with an extended APD, either due to enhanced depolarization or reduced repolarization. LQTS increases the risk of developing a unique cardiac arrhythmia known as Torsades de Pointes (TdP), identified by a twisting of the QRS complex around the isoelectric line on the ECG (Surawicz, 1989). TdP can revert to a normal sinus rhythm or develop into further complications such as syncope, ventricular fibrillation, or sudden cardiac death (Vincent *et al.*, 1992; Sanguinetti & Tristani-Firouzi, 2006). LQTS is classified as genetic (inherited) or acquired (environmental). To date, roughly 30 types of LQTS have been discovered, which are associated with over 400 mutations in genes encoding the pore-forming α -subunits of ion channels or their associated proteins. Three clinically prominent forms of LQTS include LQTS type 1 (LQT1; $\approx 45\%$ of cases), LQTS type 2 (LQT2; $\approx 35\%$ of cases), and LQTS type 3 (LQT3; $\approx 10\%$ of cases) (Splawski *et al.*, 2000). LQT1 is associated with loss-of-function mutations in *KCNQ1*, which encodes the α -subunit of the voltage-gated K^+ channel (Kv7.1) that conducts I_{Ks} (Wang *et al.*, 1996). LQT2 is associated with loss-of-function mutations in *KCNH2*, which encodes the α -subunit of the voltage-gated K^+ channel (hERG) that conducts I_{Kr} (Curran *et al.*, 1995). LQT3 is associated with gain-of-function mutations in *SCN5A*, which encodes the α -subunit of the voltage-gated Na^+ channel (Nav1.5) that conducts I_{Na} (Wang *et al.*, 1995).

LQT2-associated hERG mutations elicit a reduction in I_{Kr} through mechanisms involving impaired channel biosynthesis, trafficking, or gating (Zhou *et al.*, 1998a). The majority of LQT2-

hERG mutations reduce I_{Kr} through the formation of trafficking-deficient channels (Anderson *et al.*, 2006). Interestingly, some of these channels are functional when expressed on the plasma membrane. Correction of trafficking deficiency can be attained by pharmacological chaperones (Ficker *et al.*, 2002; Anderson *et al.*, 2006). Although some trafficking-deficient hERG mutants can be rescued pharmacologically, the tendency of most chaperones to block hERG channels eliminates any therapeutic potential *in vivo* (Ficker *et al.*, 2002).

In addition to genetic onset, LQTS can be acquired in nature. A large spectrum of medications, including those used to treat arrhythmias, can induce LQTS and promote TdP (Sanguinetti & Tristani-Firouzi, 2006). The hERG channel is susceptible to drug-induced block by antiarrhythmic, antihistamine, psychiatric, and antimicrobial compounds. These highly potent hERG blockers include, but are not limited to E4031, dofetilide, quinidine, astemizole, and cisapride (Keating & Sanguinetti, 2001). Due to the propensity of non-specific hERG channel blockage, it is common to screen the impact of newly developed compounds on hERG activity to prevent drug-induced LQTS (Sanguinetti & Tristani-Firouzi, 2006).

1.2 The hERG K^+ Channel

1.2.1 Structure

The *human ether-a-go-go related gene* (*hERG*) or *KCNH2* encodes the pore-forming α -subunit of the voltage-gated K^+ channel (hERG), which conducts the rapidly activating delayed rectifier K^+ current (I_{Kr}) (Sanguinetti *et al.*, 1995). As previously mentioned, the hERG channel plays an important role in phase 3 of the ventricular action potential by eliciting significant repolarization. The hERG channel is described as a homotetramer comprised of four identical α -subunits. Similar to other voltage-gated K^+ channels, each hERG subunit contains six transmembrane segments, denoted S1 – S6 (Trudeau *et al.*, 1995) (Figure 2A). Segments S1 – S4

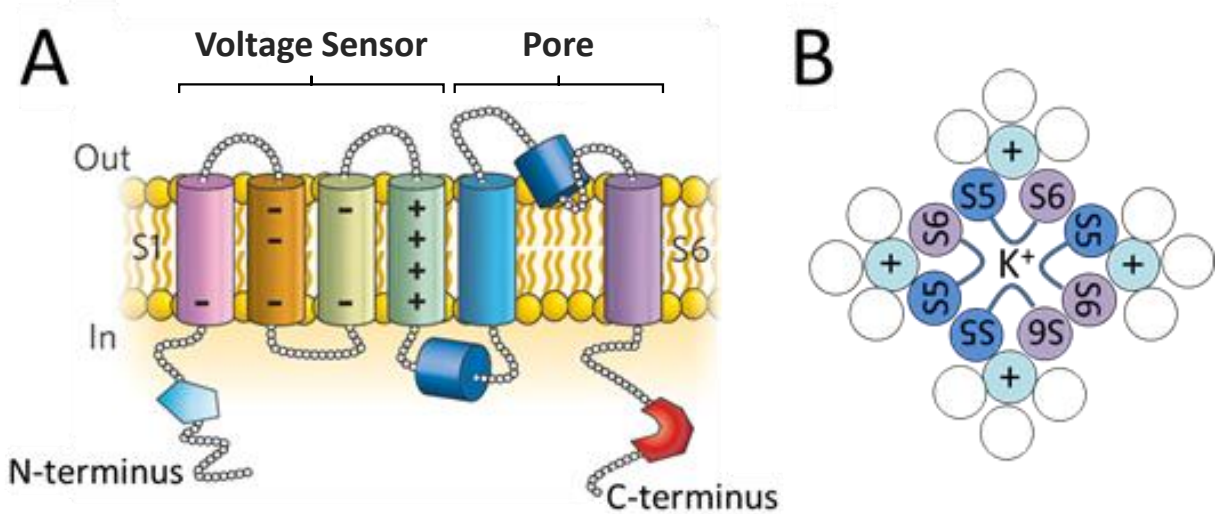


Figure 2. Schematics of hERG channel structure.

(A) Diagram of a single hERG channel subunit. Each cylinder represents one transmembrane domain (S1 to S6 from left to right). S1 to S4 constitute the voltage sensor with S4 domain carrying 6 positively charged amino acids. S5 and S6 form the pore conducting K^+ current. The N-terminal Per-Arnt-Sim (PAS) domain (light blue pentagon), C-terminal cyclic nucleotide binding (cNDB) domain (red polygon), S4-S5, and S5-pore linkers (blue cylinders) are also indicated. Modified from Sanguinetti & Tristani-Firouzi, 2006. (B) Diagram of 4 subunits of hERG forming a Kv11.1 channel. These subunits are oriented with pore domains facing towards each other to form the ion conduction pathway. The positively charged S4 domain, and pore-forming S5 and S6 domains are denoted in colors corresponding to those in panel (A).

comprise the voltage sensor domain, where the S4 segment contains several positively charged amino acid residues. Fluctuations in the membrane potential cause the S4 segment to move, resulting in conformational changes that activate or deactivate the channel (Smith & Yellen, 2002). Segments S5 – S6 comprise the pore domain that forms the ion conduction pathway. The pore loop, located between the S5 and S6 segments, confers selectivity for K⁺ ions (Doyle *et al.*, 1998). In functional channels, the pore domain of each subunit lines the pathway that selectively conducts K⁺ ions (Figure 2B).

1.2.2 Kinetics and Gating

Unique to other voltage-gated K⁺ channels, hERG exists in three conformational states: closed (non-conducting), open (conducting), and inactivated (non-conducting) (Sanguinetti & Tristani-Firouzi, 2006) (Figure 3A). The transition between each conformation is voltage-dependent. Transition between the closed and open conformations is slow, while transition between the open and inactivated conformations is rapid (Sanguinetti & Tristani-Firouzi, 2006). As a result, hERG channels display a unique current profile in response to changing voltages (Figure 3B). At negative membrane potentials (-80 mV), hERG channels are in the closed conformation. Following depolarization (positive to -60 mV), hERG channels slowly open before rapidly inactivating, resulting in a small outward K⁺ current. Increasing depolarization to more positive membrane potentials results in more channels opening and subsequently inactivating. When repolarization is initiated, hERG channels rapidly recover from inactivation to produce a large outward K⁺ current, resulting in profound repolarization before entering a closed state. This is referred to as the “peak tail current”, which reflects the current conducted by functional channels expressed in the plasma membrane (Vandenberg *et al.*, 2012). The rate of repolarization decreases over time due to closing channels and reduced equilibrium potential of

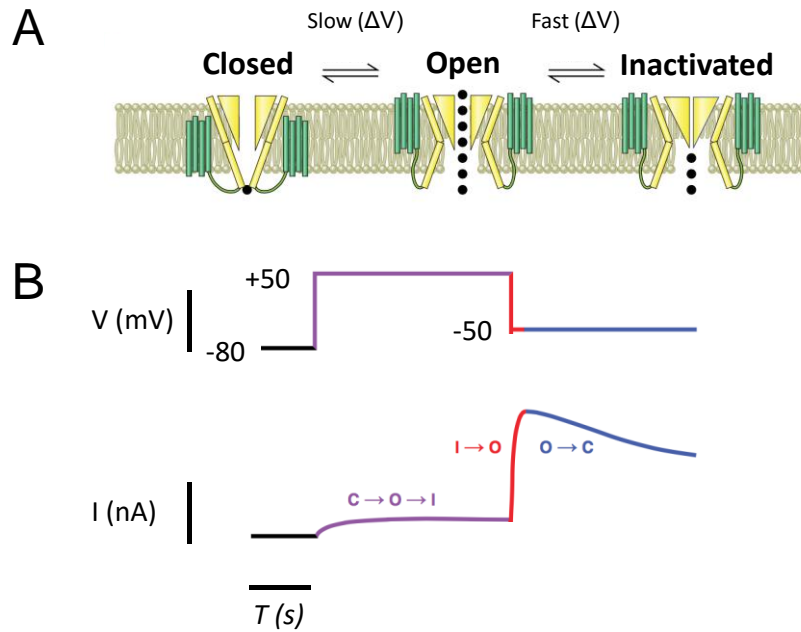


Figure 3. Gating kinetics of hERG channels.

(A) hERG channels exist in one of three conformational states: closed (non-conducting), open (conducting), or inactivated (non-conducting). The transition between each conformation is voltage dependent. Transition between the closed and open conformations is slow, while transition between the open and inactivated conformations is rapid. At negative membrane potentials (-80 mV) hERG channels are closed. Upon depolarization (+50 mV) hERG channels open before rapidly inactivating. Repolarization (-50 mV) results in rapid recovery from inactivation followed by slow closing of the channels. (B) Voltage protocol and corresponding current elicited by cell surface hERG channels. Modified from Vandenberg *et al.*, 2012.

K⁺ ions. These unique gating properties of hERG are essential for maintaining the plateau (phase 2) in the ventricular action potential (Perrin *et al.*, 2008). The slow opening and rapid inactivation of hERG channels at depolarized membrane potentials produces a small K⁺ current, providing adequate time for the plateau phase to occur. Furthermore, the slow rate of channel closing suppresses early afterdepolarizations, preventing the onset of premature beats (Lu *et al.*, 2001).

1.2.3 Biosynthesis and Trafficking

The synthesis of hERG channels begins with the translation of mRNAs into polypeptides, which are translocated into endoplasmic reticulum (ER). Folding of nascent hERG polypeptides and assembly into tetramers is assisted by molecular chaperones in the ER or cytosol (Ficker *et al.*, 2003). Chaperones remain bound to hERG proteins until a native structure is achieved. Upon proper folding and dissociation of chaperones, each subunit undergoes asparagine (N)-linked glycosylation, before channels are trafficked to the Golgi apparatus. Mutant channels that improperly fold remain bound to chaperones and are retained in the ER (Ficker *et al.*, 2003; Wang *et al.*, 2012). Prior to N-linked glycosylation, nascent hERG proteins have a molecular weight of 132 kDa (Zhou *et al.*, 1998a). Individual hERG proteins contain one consensus site for N-linked glycosylation (N598) (Gong *et al.*, 2002). Core-glycosylation involves the addition of a mannose oligosaccharide to form immature hERG proteins with a molecular weight of 135 kDa. Interestingly, glycosylation of N598 is not required for trafficking of functional channels to the cell surface; however, it seems to enhance channel stability (Gong *et al.*, 2002). Site-directed mutagenesis of N598 reduces the half-life of hERG protein, but does not abolish hERG current (Gong *et al.*, 2002). Following glycosylation, channels are trafficked to the Golgi apparatus where immature hERG proteins undergo complex glycosylation to form mature hERG proteins

with a molecular weight of 155 kDa (Zhou *et al.*, 1998a). Fully-glycosylated, mature hERG proteins are then transported to the plasma membrane as functional channels with a half-life of roughly 11 hours (Ficker *et al.*, 2003). These mature hERG channels display sensitivity toward extracellular proteinase K, whereas immature hERG channels are resistant (Zhou *et al.*, 1998a). Thus, 155-kDa proteins represent mature channels on the cell surface, while 135-kDa proteins represent immature channels inside the cell. This discrepancy in molecular weight provides a convenient assay for Western blot analysis of hERG.

A major determinant of hERG function is the density of channels on the cell surface. Expression at the cell surface is regulated by a balance between anterograde trafficking to- and retrograde trafficking from- the plasma membrane. These processes are tightly controlled to maintain homeostatic expression of hERG channels and to ensure optimal function.

1.2.4 Internalization and Degradation

Endocytosis of transmembrane proteins occurs through clathrin-dependent or clathrin-independent pathways (Doherty & McMahon, 2009). Mechanisms of clathrin-independent pathways include, caveolin-mediated endocytosis, macropinocytosis, and phagocytosis (Hansen & Nichols, 2009). Caveolae are plasma membrane pits that form lipid-raft domains to facilitate endocytosis (Parton & Simons, 2007). Integral membrane proteins known as caveolins are the principal component of caveolae. Caveolins oligomerize to form the membrane pit and act as scaffolds for the recruitment of signaling molecules (Parton & Simons, 2007). Three caveolin isoforms have been identified in mammalian cells (Cav1, Cav2, and Cav3) (Rothberg *et al.*, 1992; Scherer *et al.*, 1996). Cav1 and Cav2 are ubiquitously expressed, particularly rich in non-muscle tissues, whereas Cav3 is expressed in cardiac, skeletal, and smooth muscle cells (Parton & Simons, 2007). In the context of hERG channels, endocytosis occurs through a caveolin-

mediated pathway. Our lab has previously demonstrated that cell surface expression of hERG channels is regulated by Cav3 through the E3 ubiquitin ligase Nedd4-2. During endocytosis, Cav3, hERG, and Nedd4-2 form a complex at the plasma membrane. Overexpression of Cav3 enhances the interaction between Nedd4-2 and hERG channels, leading to a concomitant increase in channel ubiquitination and degradation (Guo *et al.*, 2012).

Cell surface expression of hERG channels is also dependent on the composition of the extracellular environment. In particular, extracellular K^+ has shown to play a crucial role in the stability of hERG channels at the plasma membrane. Our lab found that reduced extracellular K^+ concentration (hypokalemia; lower than 3.5 mM) accelerated hERG internalization and ubiquitination (Guo *et al.*, 2009). Low K^+ -induced degradation of hERG channels was later shown to occur through Cav1- and Cav3-mediated endocytosis (Massaeli *et al.*, 2010).

1.3 Rab GTPases

The movement of transmembrane proteins, between the plasma membrane and intracellular compartments, is carried out by small transport vesicles that bud from donor compartments and fuse with acceptor compartments. The mechanisms underlying this process can be divided into four major steps: (1) vesicle formation, (2) vesicle motility, (3) vesicle docking, and (4) vesicle fusion to the target compartment (Hutagalung & Novick, 2011). Rab GTPases are key components of transport vesicles, which contribute to the regulation of intracellular trafficking at each of the four major steps. Rab proteins are a subfamily of small monomeric GTPases (20 – 29 kDa) ubiquitously expressed in mammalian cells (Pereira-Leal & Seabra, 2000). To date, more than 60 types of Rab proteins have been identified (Schultz *et al.*, 2000).

Throughout the trafficking process Rab GTPases translocate between the cytosol and the membrane of transport vesicles (Hutagalung & Novick, 2011). Membrane insertion requires the addition of geranyl geranyl groups on two carboxyl-terminal cysteine residues (C-C or C-X-C) by Rab geranylgeranyl transferase (Alexandrov *et al.*, 1994). Rab GTPases function as molecular switches, cycling between the GDP-bound (inactive) and GTP-bound (active) states. This switch is governed by guanine nucleotide exchange factors (GEFs), which remove GDP to allow for GTP binding, and GTPase-activating proteins (GAPs), which enhance the intrinsic hydrolysis of GTP into GDP (Grosshans *et al.*, 2006). In the inactive state, Rab GTPases are bound by GDP dissociation inhibitors (GDIs) that conceal the geranyl geranyl group, resulting in cytosolic retention (Rak *et al.*, 2003). However, GDI displacement factors (GDFs) promote the release of GDIs to allow for membrane insertion and subsequent activation by GEFs (Sivars *et al.*, 2003). In the active state, membrane-bound Rab GTPases interact with specific effectors that confer a particular function in the trafficking of vesicles (Grosshans *et al.*, 2006). Upon inactivation by GAPs, Rab GTPases are extracted by GDIs and recycled back into the cytosol for subsequent trafficking events.

Rab GTPases are organized into distinct intracellular compartments, conferring unique roles for different Rab proteins. The specificity of localization is established through local activation by GEFs and recruitment of effectors that indirectly prevent membrane extraction by GDIs (Grosshans *et al.*, 2006; Stenmark, 2009). The organization of Rab proteins has led to the characterization of several noteworthy endosomal compartments (Figure 4): early endosomes contain Rab5 and Rab4 populations; recycling endosomes contain Rab4 and Rab11 populations; late endosomes contain Rab7 and Rab9 populations (Soldati *et al.*, 1995; Sönnichsen *et al.*, 2000).

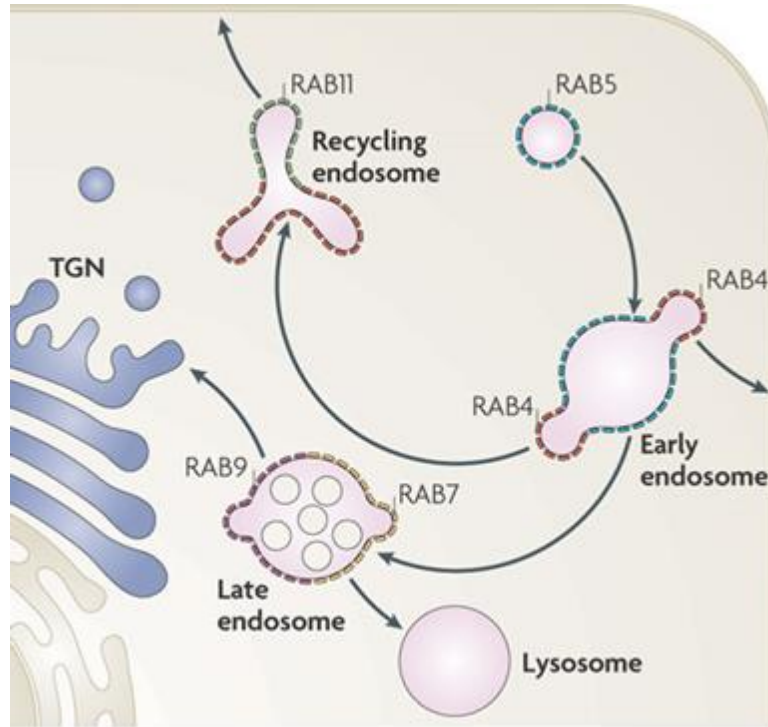


Figure 4. Rab compartmentalization and Rab domains within endosomes.

Occurrence of microdomains enriched for specific Rab GTPases, as exemplified with endosomes. Early endosomes contain separate domains enriched in RAB5 (blue) and RAB4 (red), which are involved in endosome fusion and endocytic recycling, respectively. The recycling endosome contains domains enriched in RAB4 and RAB11 (green), which are involved in vesicle trafficking from the early endosome and to the plasma membrane, respectively. Late endosomes contain domains enriched in RAB7 (yellow) and RAB9 (purple), which mediate trafficking to lysosomes and the *trans*-Golgi network (TGN), respectively. Modified from Stenmark, 2009.

In regards to their function: Rab5 mediates fusion of endocytic vesicles from the plasma membrane with early endosomes (Bucci *et al.*, 1992); Rab 4 mediates fast recycling from early endosomes to the plasma membrane (van der Sluijs *et al.*, 1992); Rab7 mediates the transport of late endosomes to lysosomes, while Rab9 directs late endosomes to the trans-Golgi network (TGN) (Lombardi *et al.*, 1993; Vanlandingham & Ceresa, 2009); Rab11 mediates the slow transport of recycling endosomes to the plasma membrane (Ullrich *et al.*, 1996).

The cell surface expression of ion channels is regulated by the action of Rab GTPases at various steps in the trafficking process (Pochynyuk *et al.*, 2007). Ion channel function is dependent on cell surface expression, which is not only regulated by anterograde and retrograde trafficking, but also through recycling of internalized channels back to the plasma membrane. More specifically, Rab GTPases have been implicated in the trafficking of cardiac K⁺ channels, including Kv1.5, Kv7.1, and hERG. In both HEK293 cells and cardiac myoblasts, Zadeh *et al.* (2008) have demonstrated that Kv1.5 channels internalize with Rab5, and subsequently recycle to the plasma membrane with Rab4 and Rab11. Interestingly, recycling via Rab4 was a fast process (10 min), whereas recycling via Rab11 was a slow process (24 h). Similar findings were reported for Kv7.1, where internalization was Rab5-dependent and recycling was Rab11-dependent (Seeböhm *et al.*, 2007). Of particular interest to this study, the homeostatic expression of hERG channels in the plasma membrane is regulated by Rab11. A dominant-negative Rab11 mutant was found to decrease cell surface expression of hERG channels and impair Golgi processing (maturation from 135 kDa to 155 kDa) (Delisle *et al.*, 2009). Our lab has confirmed this finding, demonstrating that hERG channels are recycled to the plasma membrane by Rab11 in physiological (5 mM extracellular K⁺) and pathophysiological (lower than 3.5 mM extracellular K⁺) conditions (Chen *et al.*, 2015). Furthermore, knockdown of Rab11 function, but

not Rab4, with a dominant-negative mutant reduced hERG expression and current. We have also shown that serum glucocorticoid-inducible kinase 1 (SGK1) and SGK3 enhance mature hERG expression partly by promoting Rab11-dependent recycling (Lamothe & Zhang, 2013). Together these findings strongly characterize the role of Rab11 in mediating hERG channel trafficking and maintaining homeostatic expression in the plasma membrane.

1.4 Phosphoinositide 3-kinase (PI3K) Signaling

Phosphatidylinositols (PtdIns) are phospholipids that comprise a phosphoglyceride linked to the hydroxyl group of an inositol ring. The inositol ring can be phosphorylated and dephosphorylated at several positions by various lipid kinases and phosphatases, respectively (Vanhaesebroeck *et al.*, 2001). Phosphoinositide 3-kinase (PI3K) is a lipid kinase responsible for converting PtdIns(4,5)P₂, its primary target, into PtdIns(3,4,5)P₃ (Stephens *et al.*, 1993). Conversely, PtdIns(3,4,5)P₃ can be converted by the lipid phosphatase, PTEN (phosphatase and tensin homologue deleted on chromosome 10), which functions as 3'-phosphatase to produce PtdIns(4,5)P₂ (Maehama & Dixon, 1998).

PI3Ks are evolutionarily conserved lipid kinases that mediate cell growth, proliferation, and apoptosis, in both physiological and pathophysiological states (Oudit & Penninger, 2009). Three classes of PI3K have been identified based on their mode of activation, structure, and substrate specificity (Oudit & Penninger, 2009). Class I PI3Ks are of particular interest, due to their well-characterized role in cardiovascular physiology. Typically, the activation of class I PI3Ks occurs through the stimulation of receptor tyrosine kinases (RTKs; class I_A) or G protein-coupled receptors (GPCRs; class I_B). Class I_A and I_B PI3Ks are heterodimers composed of a catalytic subunit and a regulatory adaptor subunit. Class I_A catalytic subunits include p110 α ,

p110 β , and p110 δ , which are associated with the p85 α , p85 β , and p55 γ regulatory subunits, respectively (Foster *et al.*, 2003). The class I_B catalytic subunit, p110 γ , tightly associates with its regulatory subunit, p101 γ (Foster *et al.*, 2003). Although class I catalytic subunits are widely expressed in tissues, the p110 α , p110 β , and p110 γ isoforms are notably expressed in the heart, specifically cardiomyocytes (Schlüter *et al.*, 1999; Shioi *et al.*, 2000; Crackower *et al.*, 2002). The expression pattern of regulatory subunits mirrors their corresponding catalytic subunits. Class I_A regulatory subunits contain two Src-homology 2 (SH2) domains that recognize phosphorylated tyrosine residues (Y-X-X-M) on stimulated RTKs, facilitating the recruitment of PI3K kinases to the plasma membrane for phosphorylation (Burke & Williams, 2013). Conversely, the class I_B catalytic and regulatory subunits bind to G $\beta\gamma$ dimers following GPCR stimulation, also leading to the recruitment of PI3K from the cytosol to the plasma membrane (Brock *et al.*, 2003). Phosphorylation of Class I PI3K regulatory subunits relieves constitutive inhibition on the catalytic subunit, resulting in activation of the kinase (Cuevas *et al.*, 2001). Thus, translocation from the cytosol to the plasma membrane promotes class I PI3K-dependent phosphorylation of PtdIns(4,5)P₂ (Oudit & Penninger, 2009).

The antagonistic effect of PTEN on PI3K is evolutionarily conserved in many cell types, including cardiomyocytes (Crackower *et al.*, 2002). Mammalian PTEN is 50 – 60 kDa and is comprised of a N-terminal polybasic tail and phosphatase domain, a C2 domain, and a C-terminal tail with putative phosphorylation sites (Lee *et al.*, 1999; Leslie & Downes, 2002). The main physiological target of PTEN is membrane-bound PtdIns(3,4,5)P₃. Due to constitutive phosphorylation of C-terminal residues, PTEN is retained in an inactive state within the cytosol (Das *et al.*, 2003). Activation involves dephosphorylation and recruitment to the plasma membrane via electrostatic interactions between the phosphatase/C2 domain and PtdIns(4,5)P₂.

1.4.1 PI3K-dependent Activation of Akt

The balance of PtdIns(4,5)P₂ and PtdIns(3,4,5)P₃ membrane expression is predominantly regulated by PI3K and PTEN (Oudit & Penninger, 2009). This balance is a key mediator of PI3K-dependent signaling. The generation of PtdIns(3,4,5)P₃ results in membrane recruitment and selective activation of downstream effectors. By binding to a common pleckstrin homology (PH) domain, PtdIns(3,4,5)P₃ co-localizes phosphoinositide-dependent kinase-1 (PDK1) with kinase substrates, such as Akt (also known as protein kinase B; PKB), resulting in their phosphorylation and activation (Alessi *et al.*, 1997; Bellacosa *et al.*, 1998). PDK1 is a ubiquitously expressed 67 kDa monomer containing a N-terminal kinase domain and a C-terminal PH domain (McManus *et al.*, 2004). Mutagenesis studies have shown that the PH domain of PDK1 is crucial for the activation of Akt, which in turn is dependent on the PI3K-mediated production of PtdIns(3,4,5)P₃ in the plasma membrane (Biondi *et al.*, 2001; McManus *et al.*, 2004).

Protein kinase B (PKB) or Akt is a serine/threonine kinase that mediates many cellular processes, including cell metabolism, growth, proliferation, and survival (Liao & Hung, 2010). It is a member of the AGC kinase subfamily, which includes protein kinase A (PKA), protein kinase G (PKG), protein kinase C (PKC), and the serum and glucocorticoid-inducible kinase (SGK). There are three isoforms of Akt, including Akt1 (PKB α), Akt2 (PKB β), and Akt3 (PKB γ), all of which are ubiquitously expressed in mammalian cells (Liao & Hung, 2010). Structurally, Akt comprises a N-terminal PH domain, a central catalytic domain, and a C-terminal regulatory domain that contains a hydrophobic motif, which is characteristic of AGC kinases (Hanada *et al.*, 2004). The full activation of Akt occurs through a sequential multi-step process. Akt is first recruited to the plasma membrane where it co-localizes with PDK1 through

an interaction between its PH domain and PtdIns(3,4,5)P₃ (Bellacosa *et al.*, 1998). PH domain-binding induces conformational changes that allow PDK1 to phosphorylate Akt on threonine-308 in its catalytic domain (Alessi *et al.*, 1996; Milburn *et al.*, 2003). It is then phosphorylated by the rictor-mTOR complex 2 on serine-473 in its regulatory domain (Sarbasov *et al.*, 2005). Inactivation involves dephosphorylation at both residues by the serine/threonine phosphatase, protein phosphatase 2A (PP2A) (Ugi *et al.*, 2004). Mechanistically, Akt is activated upon stimulation of RTKs and GPCRs, such as the insulin receptor and muscarinic receptors (M1 and M2), respectively (Murga *et al.*, 1998; Zeng *et al.*, 2000).

1.4.2 PI3K/Akt Signaling in Cardiac Electrophysiology

PI3K/Akt signaling modulates electrical activity within the heart through the regulation of several ion channels (Oudit & Penninger, 2009). Myocardium or isolated cardiomyocyte stimulation by insulin-like growth factor-1 (IGF-1) has been shown to increase L-type Ca²⁺ channel currents (I_{Ca-L}) and contractility via PI3K-dependent activation of Akt (von Lewinski *et al.*, 2003; Sun *et al.*, 2006). The role of PI3K/Akt signaling has also been implicated in the regulation of hERG channel function. Basal Akt activation is required for normal hERG channel function in human embryonic kidney (HEK293) cells (Zhang *et al.*, 2003). Furthermore, basal active Akt levels are mediated through both PI3K-dependent and PI3K-independent pathways (Zhang *et al.*, 2003). Akt controls a variety of cellular processes through its activity on multiple downstream substrates (Manning & Cantley, 2007). A substrate of interest in our studies is phosphatidylinositol 3-phosphate 5-kinase (PIKfyve), a lipid kinase implicated in endosomal trafficking. PIKfyve localizes to endosomal compartments via its FYVE domain (Gillooly *et al.*, 2000; Sbrissa *et al.*, 2002), where it phosphorylates PtdIns(3)P to produce PtdIns(3,5)P₂ (Sbrissa *et al.*, 1999). In a PI3K-dependent manner, Akt phosphorylates PIKfyve on serine-318, resulting

in enhanced production of PtdIns(3,5)P₂ within endosomal vesicles (Berwick *et al.*, 2004). This mechanism is responsible for the insulin-induced increase of glucose transporter 4 (GLUT4), where trafficking of GLUT4 was promoted in response to increased PtdIns(3,5)P₂ production (Berwick *et al.*, 2004). Interestingly, Akt-mediated activation of PIKfyve enhances hERG current, although through an unknown mechanism (Pakladok *et al.*, 2013). The activity of PIKfyve and production of PtdIns(3,5)P₂ have also been linked with Rab-mediated endosomal trafficking. Seebohm *et al.* (2007) have demonstrated that SGK1, a close relative of Akt, increases cell surface expression of Kv7.1 channels by promoting Rab11-mediated recycling to the plasma membrane. SGK1-mediated phosphorylation of PIKfyve led to increased PtdIns(3,5)P₂ in Rab endosomes, which may act as a positive effector for the Rab11 GTP-bound (active) state (Seebohm *et al.*, 2007).

1.5 β -arrestins

The arrestin family of proteins is comprised of four isoforms (arrestin 1 – 4). Arrestin 1 and 4 comprise the visual arrestins, which display restricted expression in retinal rods and cones (Pfister *et al.*, 1985). Conversely, arrestin 2 (β -arrestin-1) and arrestin 3 (β -arrestin-2) are ubiquitously expressed and share 78% sequence homology (Attramadal *et al.*, 1992). Although discovered for their ability to desensitize G protein-coupled receptors (GPCRs), β -arrestins have since been shown to act as multiprotein scaffolds to mediate receptor endocytosis and G protein-independent signaling (DeWire *et al.*, 2007).

1.5.1 Traditional GPCR Signaling

G protein-coupled receptors (GPCRs) represent the most physiologically diverse and versatile family of membrane receptors, ubiquitously expressed in mammalian cells (Lee *et al.*, 2001; Takeda *et al.*, 2002). They are characterized by a conserved structural motif of seven

transmembrane-spanning domains and interact with a wide variety of extracellular stimuli to produce intracellular signaling cascades that elicit a physiological response (Pierce *et al.*, 2002). Consequently, they play a fundamental role in regulating many cellular processes, such as metabolism, proliferation, differentiation, and apoptosis (Pierce *et al.*, 2002). GPCRs are the most common therapeutic target in medicine and are acted upon by roughly 40% of marketed drugs (Brink *et al.*, 2004). The traditional paradigm of GPCR signaling begins with ligand binding and activation of the receptor. Stimulation of GPCRs induces conformational changes that promote the recruitment of heterotrimeric G proteins, which exchange GDP for GTP and subsequently dissociate into a G α subunit and G $\beta\gamma$ dimer. The activated G α subunits then trigger the activation of downstream effectors such as phospholipase C, adenylyl cyclase, and ion channels, which in turn generate second messengers within the cell.

1.5.2 β -arrestin-dependent Signaling

In addition to heterotrimeric G proteins, GPCRs interact with G protein-coupled receptor kinases (GRKs) and β -arrestins upon ligand binding. The GRK family of proteins is comprised of seven serine/threonine kinase isoforms (GRK 1 – 7). GRK-1 and -7 are expressed in retinal rods and cones, while GRK-4 displays limited expression in the brain, kidneys, and testes (Benovic *et al.*, 1986; Ambrose *et al.*, 1992; Weiss *et al.*, 1998). In contrast, GRK-2, -3, -5, and -6 are widely expressed in mammalian cells (Lorenz *et al.*, 1991; Parruti *et al.*, 1993; Kunapuli & Benovic, 1993; Benovic & Gomez, 1993). GRKs phosphorylate agonist-bound, activated GPCRs on serine/threonine residues in the third intracellular loop and C-terminal tail region (Reiter & Lefkowitz, 2006). Phosphorylation leads to the recruitment of β -arrestins, the specificity of which varies between different GPCRs (Reiter & Lefkowitz, 2006). The receptor- β -arrestin interaction has been displayed in many GPCRs, including the β_2 -adrenergic receptor (β_2 AR),

angiotensin II type 1 receptor (AT₁R), and muscarinic receptors (M2 and M3) (Roseberry & Hosey, 2001; Ahn *et al.*, 2004; Novi *et al.*, 2005; Shenoy *et al.*, 2006). The pattern and degree of C-terminal phosphorylation is suggested to govern the stability of the receptor- β -arrestin complex, which has established two classes of GPCRs (Oakley *et al.*, 2000, 2001): Class A receptors form a weak, transient interaction with β -arrestin and undergo rapid recycling following dissociation (β_2 AR); Class B receptors form a strong, prolonged interaction with β -arrestin and undergo slow recycling as a complex (AT₁R).

The ability of β -arrestins to scaffold signaling complexes provides a greater degree of diversity in GPCR signal transduction. Among several β -arrestin-dependent pathways, the activation of extracellular signal-regulated kinase 1 (ERK1) and ERK2 via AT₁R is best characterized. The utilization of PKC inhibitors (G protein inhibition) or β -arrestin siRNA following AT₁R stimulation has delineated independent mechanisms of ERK1/2 activation by G proteins and β -arrestins (Wei *et al.*, 2003). Further investigation has shown that G protein-dependent ERK activation is rapid (peak 2 min) and transient ($t_{1/2} = 2$ min), while β -arrestin-dependent ERK activation is slow (peak 10 min) and persistent ($t_{1/2} = 60$ min) (Ahn *et al.*, 2004). Similar characteristics of ERK1/2 activation have been identified following β_2 AR stimulation (Shenoy *et al.*, 2006). The temporally distinct activation of ERK1/2 by G proteins and β -arrestins suggests unique physiological outcomes for each pathway. β -arrestin signaling has also been associated with the receptor tyrosine kinase, insulin-like growth factor-1 receptor (IGF1-R), where stimulation by IGF1 promotes PI3K activation and Akt phosphorylation. In mouse embryo fibroblasts lacking both β -arrestin-1 and -2, IGF1 was unable to elicit Akt phosphorylation (Povsic *et al.*, 2003). However, transfection with β -arrestin-1 restored PI3K

activity and Akt phosphorylation (Povsic *et al.*, 2003). Due to the novelty of β -arrestin-mediated signaling, the role of β -arrestins in the regulation of hERG channels remains to be elucidated.

1.6 Designer Receptors Exclusively Activated by Designer Drugs (DREADDs)

The complexity and diversity of GPCR signaling makes it difficult to analyze or manipulate their distinct pathways (Hermans, 2003). It is well understood that stimulation of GPCRs by various ligands leads to G protein- and β -arrestin-dependent signaling pathways with unique physiological outcomes. Complexity is furthered by the existence of multiple G protein and β -arrestin isoforms. Moreover, heterologous expression of GPCR subtypes that are activated by a single ligand impairs the interpretation of physiological responses (Wess *et al.*, 2013; Thiel *et al.*, 2013). The development of designer receptors exclusively activated by designer drugs (DREADDs), which lack constitutive activity and are unresponsive to endogenous ligands, has allowed for the selective activation of GPCR subtypes by otherwise pharmacologically inert compounds (Thiel *et al.*, 2013). These designer receptors circumvent the problem associated with multi-ligand activation, complex signaling, and heterologous expression of GPCRs in cells and tissues (Wess *et al.*, 2013). The most commonly used designer receptor is the mutant muscarinic M3 designer receptor (M3D). Point mutations in the extracellular third and fifth transmembrane domains (Y148C and A238G) prevent binding with the endogenous ligand acetylcholine and allow for exclusive activation by clozapine-*N*-oxide (CNO) (Armbruster *et al.*, 2007). Upon CNO stimulation, M3D carries out both G_q protein and β -arrestin signaling in a similar fashion to wild type M3 receptors (Alvarez-Curto *et al.*, 2011). More recently, Nakajima & Wess (2012) introduced a third point mutation (R165L) to develop an arrestin-biased M3D (M3D-arr), which displays impaired G_q protein-coupling and exclusive β -arrestin activation (Figure 5). M3D-arr represents a powerful tool for the exclusive study of β -arrestin signaling.

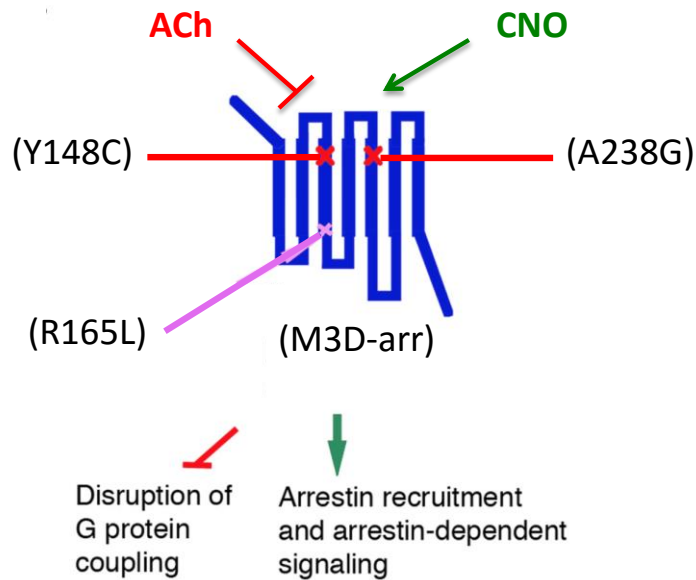


Figure 5. Structure of arrestin-biased M3 designer receptor (M3D-arr).

Structure of the arrestin-biased M3 receptor (M3D-arr) that cannot activate heterotrimeric G proteins but is able to initiate arrestin-mediated signaling. The M3D-arr designer receptor contains the Y148C and A238G point mutations in TM3 and TM5, respectively (indicated by the red x marks) and is unable to bind acetylcholine (ACh). In addition, the rM3Darr construct contains the R165L point mutation at the bottom of TM3 (indicated by the purple x mark). Introduction of this point mutation into the wild type M3R virtually abolishes productive receptor-G protein coupling. As a result, clozapine-*N*-oxide (CNO) treatment of M3D-arr-expressing cells does not lead to activation of heterotrimeric G proteins. However, in the presence of CNO, the M3D-arr designer receptor retains the ability to recruit β -arrestin-1 and -2 and to mediate arrestin-dependent downstream signaling. Modified from Nakajima & Wess, 2012.

Cardiac function is regulated by parasympathetic stimulation of muscarinic receptors (Harvey, 2012). Of the five muscarinic receptor subtypes (M1 – M5), M1, M2, and M3 are expressed in the heart. M3 receptor overexpression has shown to reduce the incidence of arrhythmias and sudden death associated with myocardial ischemia in mice (Liu & Sun, 2011). More specifically, M3 overexpression shortened the APD by increasing the inward rectifying K⁺ current (I_{K1}). Our lab has demonstrated that M3 receptor activation via carbachol (8 hour treatment) enhances hERG channel expression and current through G_q protein-dependent activation of PKC (Wang *et al.*, 2014). Whether β-arrestin signaling affects hERG function following M3 receptor activation remains unclear.

Hypothesis and Objectives

As mentioned in the literature review, hERG channel function is dependent on the expression of channels in the plasma membrane. Since anterograde and retrograde trafficking maintain cell surface expression, delineating mechanisms that regulate hERG trafficking is a research focus of interest. Several studies have demonstrated that Rab11 regulates homeostatic expression and function of hERG channels by facilitating endosomal recycling to the plasma membrane. Basal Akt activity, partially controlled by PI3K, is required for homeostatic hERG function. However, the mechanism through which Akt regulates hERG is unknown. Our lab has also shown that muscarinic M3 receptor signaling enhances hERG expression and current through PKC activation in a G_q protein-dependent manner. M3 receptors are also known to recruit β -arrestins upon stimulation, but the ability of β -arrestins to regulate the hERG channel has not been studied. β -arrestins scaffold a variety of downstream effectors, including PI3K, which may in fact alter hERG expression and current. Development of the arrestin-biased M3 designer receptor, M3D-arr, has allowed for the study of exclusive β -arrestin-dependent signaling. Therefore, I hypothesize that M3D-arr stimulation will enhance hERG expression and function through β -arrestin signaling, involving PI3K-dependent activation of Akt and subsequent promotion of Rab11-mediated recycling.

To examine this hypothesis, I accomplished the following objectives:

1. Study the effect of M3D-arr via CNO on hERG channel expression.
2. Study the effect of M3D-arr via CNO on hERG channel current.
3. Evaluate the interaction between M3D-arr and β -arrestin-1/2 upon CNO stimulation.
4. Determine the role of Akt in the M3D-arr mediated increase in hERG expression and to evaluate phosphorylated (activated) vs total Akt expression levels.

5. Evaluate the mechanism of Akt activation following M3D-arr activation via CNO.
6. Study the effect of M3D-arr activation via CNO on Rab11-mediated recycling of hERG.

Chapter 2: Materials and Methods

2.1 Molecular Biology

The human embryonic kidney (HEK) 293 cell line stably expressing hERG channels (hERG-HEK cells) was provided by Dr. Craig January (University of Wisconsin-Madison); hERG cDNA was provided by Dr. Gail Robertson (University of Wisconsin-Madison). The HA-tagged rat arrestin-biased M3 Designer Receptor Exclusively Activated by Designer Drugs (DREADD) [Rq(R165L); M3D-arr] plasmid was obtained from Dr. Jürgen Wess (National Institute of Diabetes and Digestive and Kidney Diseases, National Institutes of Health). The FLAG-tagged human PTEN (phosphatase and tensin homolog deleted on chromosome 10) plasmid was obtained from Xiaolong Yang (Queen's University). The Rab11 dominant-negative (DN) mutant (Rab11 S25N) plasmid was obtained from Addgene (Cambridge, Massachusetts). hERG-HEK cells were maintained in normal culture medium which contained Minimum Essential Medium (MEM, Invitrogen) supplemented with 10% fetal bovine serum (FBS, Invitrogen), 1× non-essential amino acids and 1 mM sodium pyruvate, and 0.4 mg/ml G418 (Invitrogen). For transient transfections, Lipofectamine 2000 (Invitrogen) was used to transfect 2 or 8 µg of plasmid of interest into hERG-HEK cells grown in 35 mm or 100 mm cell culture dishes, respectively. Empty pcDNA3 plasmids were used as a control. For electrophysiological analyses, a GFP plasmid (pIRES2-EGFP, Clontech) was co-transfected with plasmids of interest at a ratio of 1:3 to identify transfected cells. Following transfections, cells were cultured for 24 h before experiments proceeded.

2.2 Western Blot Analysis

Whole-cell proteins were isolated from hERG-HEK cells that were transfected with plasmids of interest. Twenty-four hours after transfection, cells were cultured with treatment of interest. For protein extraction, cells were washed two times and collected in ice-cold phosphate buffered saline (PBS). Cell pellets were acquired via centrifugation at 1,500 g and aspiration of PBS supernatant. Cell pellets were then re-suspended in radioimmunoprecipitation assay (RIPA) lysis buffer containing Phenylmethylsulfonyl fluoride (PMSF, 1:100, Sigma) and a protease inhibitor cocktail (1:100, Sigma). For the detection of phosphorylated Akt, a phosphatase inhibitor (1:100, Sigma) was added to stabilize phosphorylated proteins. Whole-cell protein lysates were generated via sonication and then centrifuged at 10,000 g for 10 min to separate DNA and RNA (pellet) from protein (supernatant). Protein concentration was measured using the Bio-Rad DC Protein Assay Kit (Bio-Rad). Bovine serum albumin was used to generate standard curve (absorbance vs. concentration). Absorbance of whole-cell protein lysate was applied to standard curve to estimate concentration. Using calculated concentrations, 15 µg of protein was prepared with 5× Laemmli sample buffer. Separation of proteins was performed using sodium dodecyl sulfate polyacrylamide (8%) gel electrophoresis (SDS-PAGE). Proteins were then transferred to polyvinylidene difluoride (PVDF) membranes and blocked for 1 h using 5% non-fat milk. Membranes were incubated with primary antibodies followed by a corresponding horseradish peroxidase (HRP)-conjugated secondary antibody, each for 1 h. Incubations were followed by three 10 min washes in TBS-T (0.1% Tween-20). An enhanced chemiluminescent kit (ECL, GE Healthcare) was used to visualize proteins on Fuji X-ray films. Densitometry was performed, where optical density and area of protein bands were used to determine expression level. The expression level of actin was used as a loading control. In each

gel, the band intensities of proteins of interest were normalized to their respective actin intensities. The normalized band intensities of treatment groups were compared to respective controls and expressed as relative values.

2.3 Co-immunoprecipitation

Cells were cultured, collected, and assayed in a similar fashion to Western blot analysis procedures. For each sample, 0.5 mg of whole-cell protein in 0.5 ml lysis buffer was incubated with β -arrestin-1 or β -arrestin-2 antibodies overnight at 4° C. Glyceraldehyde 3-phosphate dehydrogenase (GAPDH) antibody was used as a negative control. The protein-antibody complexes were precipitated with protein A/G PLUS agarose beads for 4 h at 4° C. The beads were washed four times with 200 μ L of ice-cold RIPA lysis buffer and centrifuged at 10,000 *g* for 2 min. RIPA lysis buffer supernatant was aspirated after each wash. Following washes, the beads were resuspended in 50 μ L of 2 \times Laemmli sample buffer and boiled for 5 min, samples were centrifuged at 10,000 *g* for 10 min. The supernatant was collected for Western blot analyses to detect precipitated proteins.

2.4 RNA Extraction and Quantitative Reverse Transcription

Twenty-four hours after transfection of empty pcDNA3 or HA-tagged M3D-arr plasmid into hERG-HEK cells, cells were treated with or without CNO for 24 h. Total cellular RNA was then extracted from cells using a Total RNA Mini Kit (Cat No: RB050, Geneaid Biotech Ltd., Taiwan). After treatment with DNase I (Cat No: M0303S, New England BioLabs), RNA concentration was assessed using a spectrophotometer (Molecular Devices, spectra MAX plus, CA. USA).

Total RNA (1 μ g) was reverse-transcribed to cDNA using the Omniscript RT kit (Cat No: 205111, Qiagen). Quantitative reverse transcription PCR (RT-qPCR) was performed using a

thermal cycler (Model 7500, Applied Biosystems, Foster City, CA, USA) with TaqMan Gene Expression Master Mix (Cat No: 4369016, Life Technologies). GAPDH was used as a control housekeeping gene. Oligonucleotide primers were acquired from Life Technologies (hERG: Assay ID: Hs04234270_g1; GAPDH: Assay ID: Hs03929097_g1). The PCR conditions were as follows: 2 min at 50°C and 10 min at 95°C, followed by 40 cycles at 95°C for 15 s and 60°C for 1 min. Data were calculated using the $2^{-\Delta\Delta CT}$ method and are presented as fold induction of hERG transcripts normalized to GAPDH.

2.5 Immunofluorescence Microscopy

hERG-HEK cells cultured on glass coverslips were transiently transfected with empty pcDNA3 or HA-tagged M3D-arr plasmid for 24 h and then treated without (Ctrl) or with CNO. Twenty-four hours after treatment, cells were washed two times with ice-cold PBS and fixed with an ice-cold 4% paraformaldehyde-PBS solution for 15 min. The fixed cells were then permeabilized with 0.1% Triton X-100 for 10 min and blocked with 5% BSA for 1 h. To detect HA-tagged M3D-arr, a rabbit anti-HA primary antibody and an Alexa Fluor 594-conjugated donkey anti-rabbit secondary antibody were used. To detect β -arrestin-1 or β -arrestin-2, a goat anti- β -arrestin-1 or mouse anti- β -arrestin-2 primary antibody and an Alexa Fluor 488-conjugated donkey anti-goat or goat anti-mouse secondary antibody were used.

2.6 Patch Clamp Recording

The whole-cell voltage-clamp method was used to record hERG current (I_{hERG}). hERG-HEK cells were held at a holding potential of -80 mV and I_{hERG} was elicited by a series of depolarizing steps ranging from -70 to 70 mV in 10 mV increments. The depolarizing steps were followed by a repolarizing step to -50 mV to induce hERG tail currents. Current amplitude analysis of I_{hERG} was conducted using peak tail current measurements. The bath solution

contained 135 mM NaCl, 5 mM KCl, 10 mM HEPES, 10 mM glucose, 1 mM MgCl₂, and 2 mM CaCl₂ (pH 7.4 with NaOH). The internal pipette solution consisted of 135 mM KCl, 5 mM EGTA, 1 mM MgCl₂ and 10 mM HEPES (pH 7.2 with KOH).

2.7 Reagents and Antibodies

MEM, FBS, G418, non-essential amino acids, sodium pyruvate, Alexa Fluor 594-conjugated donkey anti-rabbit and Alexa Fluor 488-conjugated donkey anti-goat and goat anti-mouse secondary antibodies were purchased from Invitrogen. Rabbit anti-Kv11.1 (hERG) and anti-HA (H6908), mouse anti-FLAG (F3165), anti-HA (H3663), and anti-actin primary antibodies, electrolytes, EGTA, HEPES, glucose, BSA, Akt-1/2 kinase inhibitor (A6730) and SC79 (Akt activator; Cat No: SML0749) were purchased from Sigma-Aldrich. Goat anti-hERG (C-20) (sc-15968), anti- β -arrestin-1 (sc-9182), mouse anti- β -arrestin-2 (sc-13140) and rabbit anti-Akt (sc-1618-R) and anti-p-Akt (sc-135650) primary antibodies, as well as goat anti-mouse (sc-2005), mouse anti-goat (sc-2354), goat anti-rabbit (sc-2004) IgG-HRP secondary antibodies and protein A/G beads (sc-2003) were purchased from Santa Cruz Biotechnology. YM-201636 (PIKfyve inhibitor; Cat no: 13576) was purchased from Cayman Chemical. H7 (PKC inhibitor) was obtained from Toronto Research Chemicals (I885000). PhosSTOP phosphatase inhibitor was purchased from Roche Applied Science.

2.8 Statistical Analysis

The measurements of all results are presented as the mean \pm the standard error of the mean (S.E.M.). Two-tailed unpaired Student's *t* test or one-way ANOVA were used to determine statistical significance between treatment and control groups. A *P*-value of less than 0.05 was considered to be statistically significant.

Chapter 3: Results

3.1 CNO-mediated activation of M3D-arr increases hERG channel expression and current

The effect of arrestin-biased M3 DREADD (M3D-arr) activation via clozapine-*N*-oxide (CNO) on the hERG channel was investigated. HEK cells stably expressing hERG (hERG-HEK cells) were transfected with empty pcDNA3 (control) or M3D-arr plasmid. Twenty-four hours after transfection, cells were treated with CNO at different concentrations and for various time periods. As mentioned, the presence of Y148C, A238G, and R165L point mutations renders M3D-arr unable to bind acetylcholine and activate G proteins, but retains the ability to recruit β -arrestins in a CNO-dependent fashion (Armbruster *et al.*, 2007; Nakajima & Wess, 2012). Otherwise pharmacologically inert, CNO exclusively binds M3D-arr with high efficacy (Armbruster *et al.*, 2007). Western blot analysis was used to determine the effect of CNO-mediated activation of M3D-arr on hERG channel expression. On Western blots, hERG proteins typically display two bands with molecular masses of 135 kDa and 155 kDa. The synthesis of hERG protein occurs in the endoplasmic reticulum (ER) to form the immature, core-glycosylated channel (135 kDa), which is transported to the Golgi apparatus during trafficking to become the mature, fully-glycosylated channel (155 kDa) expressed on the plasma membrane (Zhou *et al.*, 1998*b*; Gong *et al.*, 2002). Cell surface expression is then regulated by a combination of biosynthesis, trafficking, and degradation mechanisms (Chen *et al.*, 2015; Kang *et al.*, 2015).

Treatment with 0.1, 1, and 10 μ M CNO increased mature hERG expression in M3D-arr-, but not pcDNA3-transfected cells, in a concentration-dependent manner (Figure 6A). The effect of CNO plateaued at 10 μ M and had no further effect at higher concentrations (data not shown). We then treated cells with 10 μ M CNO for various time periods. CNO caused a time-dependent increase in mature hERG expression, peaking at 24 h (Figure 6B). Furthermore, we validated the

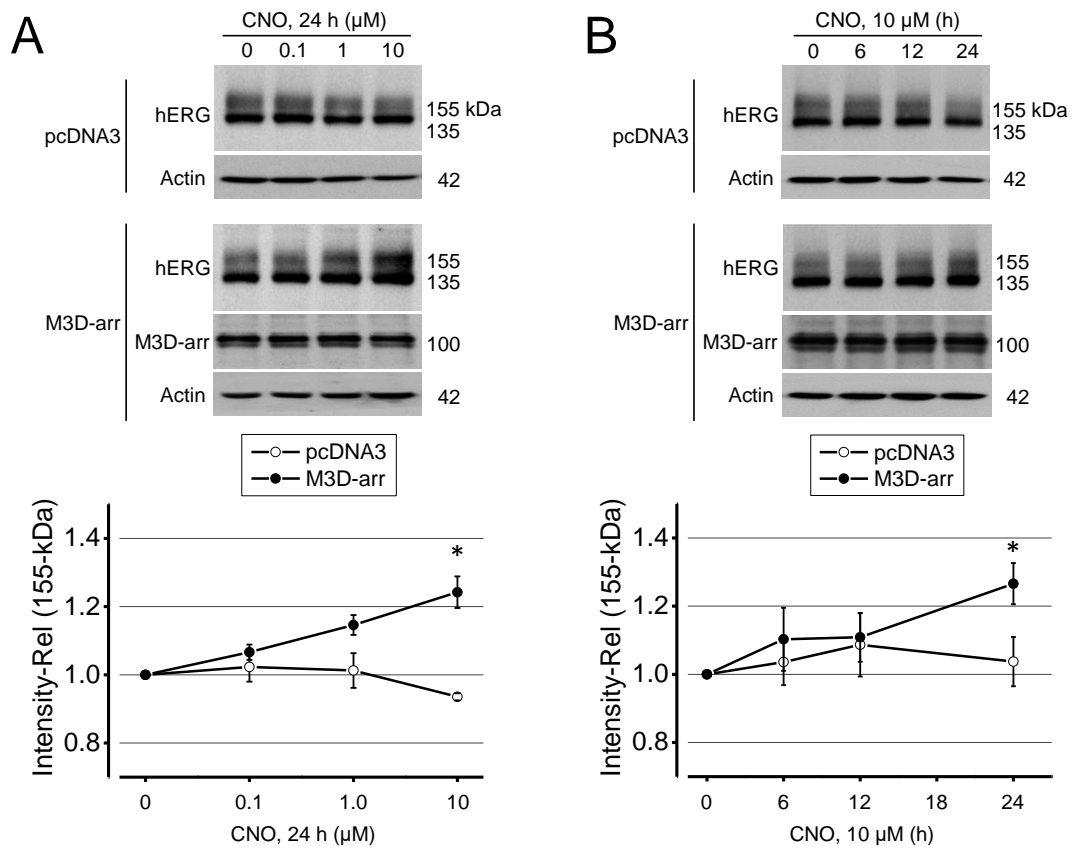


Figure 6. CNO increases mature hERG expression levels in a concentration- and time-dependent manner through M3D-arr activation.

A, Concentration-dependent effect of CNO on hERG expression (n = 3). B, Time-dependent effect of 10 μM CNO on hERG expression (n = 3). In both A and B, hERG-HEK cells were transfected with empty pcDNA3 (control) or HA-tagged M3D-arr plasmid. Twenty-four hours after transfection, cells were treated with CNO under various conditions. Whole-cell lysates were then collected for Western blot analysis. Band intensities of mature (155 kDa) hERG proteins with CNO-treatments were normalized to respective actin controls and expressed as a value relative to experimental controls in each gel. Summarized data are presented in the graphs beneath the Western blots. * $P < 0.05$ vs. Ctrl (0 μM and 0 h, respectively).

inert characteristic of CNO in the absence of M3D-arr. We found that treatment of pcDNA3-transfected cells with 10 μ M CNO for 24 h had no effect on hERG expression. Thus, for subsequent investigations in our study, we treated cells with 10 μ M CNO for 24 h, and examined the effects of M3D-arr activation on both hERG expression and current (I_{hERG}).

After establishing optimal CNO treatment, we focused on characterizing the observed increase in hERG protein expression following M3D-arr activation by CNO. Our data show that CNO significantly increased expression of mature, but not immature hERG protein, in M3D-arr-transfected hERG-HEK cells (Figure 7A). Since immature hERG protein is the intracellular precursor for mature hERG protein at the cell surface, the observed increase may be due to enhanced biosynthesis and maturation. In pursuit of delineating the mechanism of increased mature hERG expression, we performed quantitative reverse transcription PCR (RT-qPCR) on pcDNA3- and M3D-arr-transfected hERG-HEK cells cultured without (Ctrl) or with CNO. There was no significant difference in relative hERG mRNA expression between control and treatment groups (Figure 7B). Since the cell surface density of mature hERG channels is a key determinant of channel function, we hypothesized that the observed increase in expression would coincide with increased current. Parallel experiments with whole-cell patch clamp showed that CNO significantly increased I_{hERG} from 0.72 ± 0.06 nA ($n = 22$) to 1.03 ± 0.09 nA ($n = 24$) in M3D-arr-transfected cells (Figure 8A). The hERG channel is highly susceptible to drug interactions that either alter gating kinetics or completely block conductance. Thus, we plotted the tail currents against the depolarizing voltages in each cells and fitted the data to the Hill equation to obtain the conductance-voltage (g-V) relationships. In pcDNA3-transfected hERG-HEK cells, the summarized half activation voltage and the slope factor were -1.7 ± 2.5 mV and 7.9 ± 0.4 for control ($n = 11$) and -5.2 ± 2.5 mV and 8.1 ± 0.6 for CNO-treated cells ($n = 7$, $P > 0.05$). In

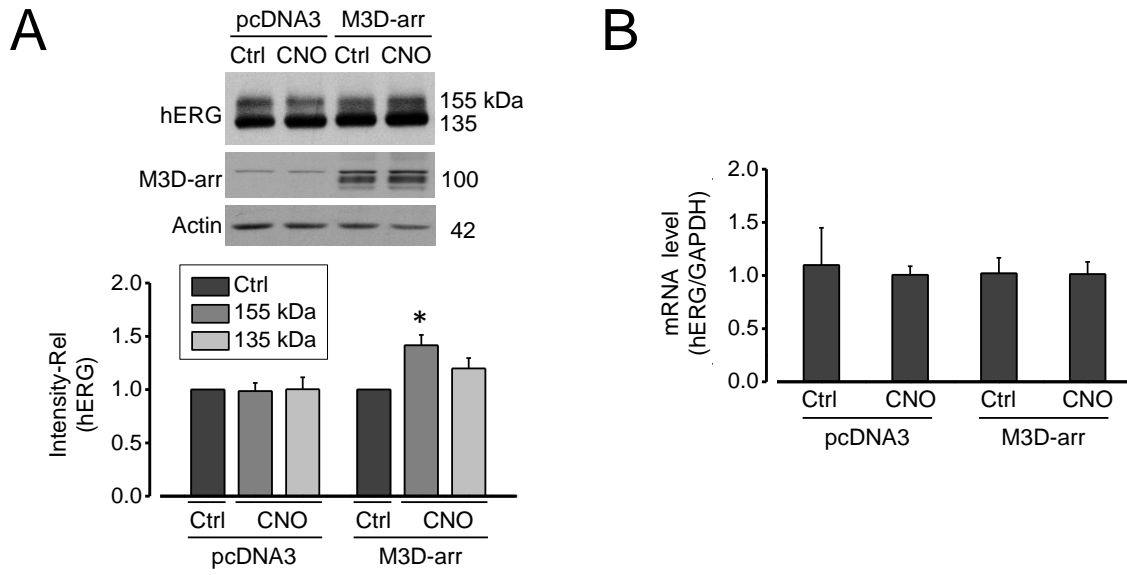


Figure 7. CNO-mediated activation of M3D-arr increases mature hERG expression levels without enhancing hERG mRNA expression.

hERG-HEK cells were transfected with pcDNA3 or HA-tagged M3D-arr plasmid. Twenty-four hours after transfection, cells were cultured without (Ctrl) or with 10 μ M CNO for 24 h. *A*, Effect of CNO-mediated M3D-arr activation on the expression of hERG channels. Band intensities of mature (155 kDa) and immature (135 kDa) hERG proteins from CNO-treated cells were normalized to respective actin controls and expressed as a value relative to experimental controls in each gel. Data from independent experiments are summarized beneath the Western blot images (pcDNA3, n = 4; M3D-arr, n = 7). *B*, Effect of CNO-mediated M3D-arr activation on relative hERG mRNA expression level. Quantitative reverse transcription PCR was conducted using mRNA from cells transfected with pcDNA3 or M3D-arr and cultured without (Ctrl) or with CNO. (pcDNA3, n = 3; M3D-arr, n = 3). GAPDH was used as a control housekeeping gene. * $P < 0.05$ vs. Ctrl.

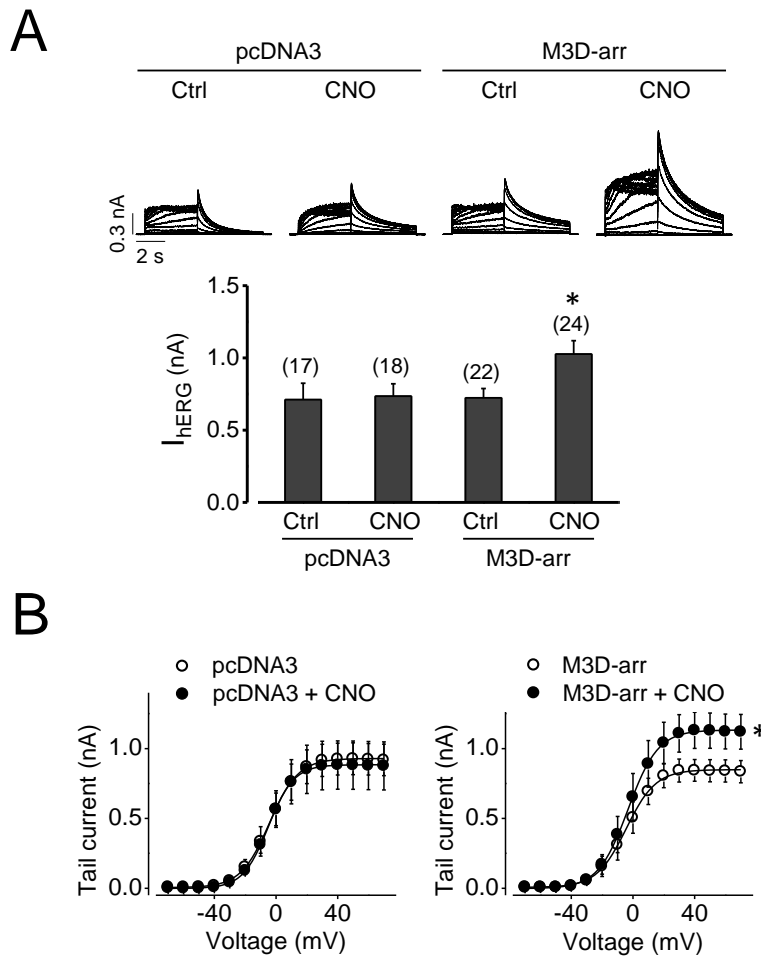


Figure 8. CNO-mediated activation of M3D-arr increases I_{hERG} .

hERG-HEK cells were transfected with pcDNA3 or HA-tagged M3D-arr plasmid. Twenty-four hours after transfection, cells were cultured without (Ctrl) or with 10 μ M CNO for 24 h. *A*, Effect of CNO-mediated M3D-arr activation on I_{hERG} . Summarized I_{hERG} is shown beneath the representative families of I_{hERG} from cells transfected with pcDNA3 or M3D-arr and cultured without (Ctrl) or with CNO. The numbers above the bars indicate the number of cells examined from 3 independent experiments. *B*, The effect of CNO mediated M3D-arr activation on the voltage-dependence of hERG channels (pcDNA3, $n = 7$ and 11; M3D-arr, $n = 11$ and 7). $*P < 0.05$ vs. Ctrl.

M3D-arr-transfected hERG-HEK cells, the half activation voltage and the slope factor were -3.8 ± 4.3 mV and 7.1 ± 0.4 for control ($n = 7$) and 0.1 ± 3.2 mV and 7.5 ± 0.3 for CNO-treated cells ($n = 11$, $P > 0.05$). Thus, CNO enhanced I_{hERG} without affecting the activation-voltage relationship of hERG channels in M3D-arr-expressed cells (Figure 8B).

3.2 CNO enhances the M3D-arr- β -arrestin interaction and co-localization at the plasma membrane.

Among four arrestin isoforms, β -arrestin-1 (arrestin 2) and β -arrestin-2 (arrestin 3) exhibit 78% amino acid sequence homology and are ubiquitously expressed in many tissues (Attramadal *et al.*, 1992; Sterne-Marr *et al.*, 1993). Following agonist binding, β -arrestins associate with GPCRs to facilitate receptor desensitization and internalization, as well as G protein-independent signaling (Goodman *et al.*, 1996; Shenoy *et al.*, 2006). β -arrestin recruitment is common to many GPCRs, including the β_2 -adrenergic receptor (β_2 -AR), angiotensin II type 1 receptor (AT₁R), muscarinic M2 receptor, and muscarinic M3 receptor (Pals-Rylaarsdam *et al.*, 1997; Ahn *et al.*, 2004; Novi *et al.*, 2005; Shenoy *et al.*, 2006). Since M3D-arr is designed to recruit β -arrestins upon CNO binding, we hypothesized that CNO enhances the M3D-arr- β -arrestin interaction which is responsible for the increase in mature hERG expression. To begin, the presence of β -arrestin-1 and -2 in this model was confirmed via Western blot analysis (data not shown). β -arrestin isoforms display varying affinity for different GPCRs (Oakley *et al.*, 2000). Therefore, we investigated whether β -arrestin-1, β -arrestin-2, or both interact with M3D-arr upon CNO treatment. To this end, co-immunoprecipitation (co-IP) experiments were performed on hERG-HEK cells transfected with M3D-arr and cultured without (control) or with CNO for 24 h (Figure 9). Specific anti- β -arrestin antibodies were used to

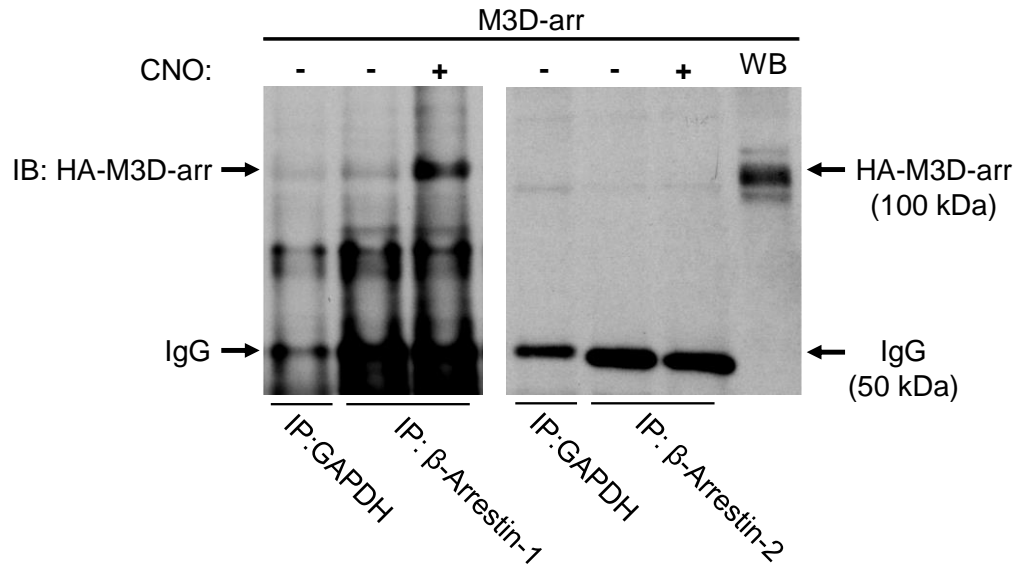


Figure 9. CNO-mediated M3D-arr activation enhances the β -arrestin-M3D-arr interaction.

Co-IP experiments illustrating that CNO-activated M3D-arr interacts with β -arrestin-1 (Left) but not with β -arrestin-2 (Right). pcDNA3 or HA-tagged M3D-arr transfected hERG-HEK cells were treated with 10 μ M CNO for 24 h. Whole-cell lysates were immunoprecipitated with an anti- β -arrestin-1 or anti- β -arrestin-2 antibody. The immunoprecipitates were immunoblotted with a rabbit anti-HA primary and goat anti-rabbit secondary antibody to detect HA-tagged M3D-arr. Anti-GAPDH was used as a negative control (n = 3 for both).

immunoprecipitate either β -arrestin-1 or -2 and associated proteins from whole-cell lysates. Precipitates were then immunoblotted with an anti-HA antibody to detect for M3D-arr. As shown in Figure 9, CNO treatment significantly enhanced the interaction between M3D-arr and β -arrestin-1, but not β -arrestin-2. Control cells displayed a faint band, which might indicate some basal level of M3D-arr- β -arrestin-1 interaction.

To examine the cellular localization of this interaction, immunocytochemical analysis was employed on hERG-HEK cells transfected with M3D-arr and cultured without (control) or with CNO for 24 h. After fixation and permeabilization, cells were incubated with anti- β -arrestin-1 or anti- β -arrestin-2 and anti-HA (to detect M3D-arr) primary antibodies. Corresponding fluorochrome-conjugated secondary antibodies were then used to visualize β -arrestin-1 or β -arrestin-2 and M3D-arr. As shown with confocal images in Figure 10A, there was increased co-localization between β -arrestin-1 and M3D-arr at the plasma membrane following CNO treatment. However, there was no increased co-localization between β -arrestin-2 and M3D-arr at the plasma membrane following CNO treatment (Figure 10B). These data are consistent with the Co-IP experiments, and indicate that M3D-arr activation via CNO enhances the interaction between M3D-arr and β -arrestin-1, specifically at the plasma membrane.

3.3 CNO-mediated activation of M3D-arr increases hERG expression through an Akt-dependent pathway.

Muscarinic M3 receptors couple with G_q proteins to activate phospholipase C, which cleaves phosphatidylinositol(4,5)biphosphate (PtdIns(4,5)P₂) to produce inositol 1,4,5-triphosphate (IP₃) and diacylglycerol (DAG) (Eglen, 2012). IP₃ stimulates the release of Ca²⁺ from the ER whereas DAG activates protein kinase C (PKC). We recently reported that M3 receptor activation via carbachol increases hERG expression through a PKC-dependent pathway

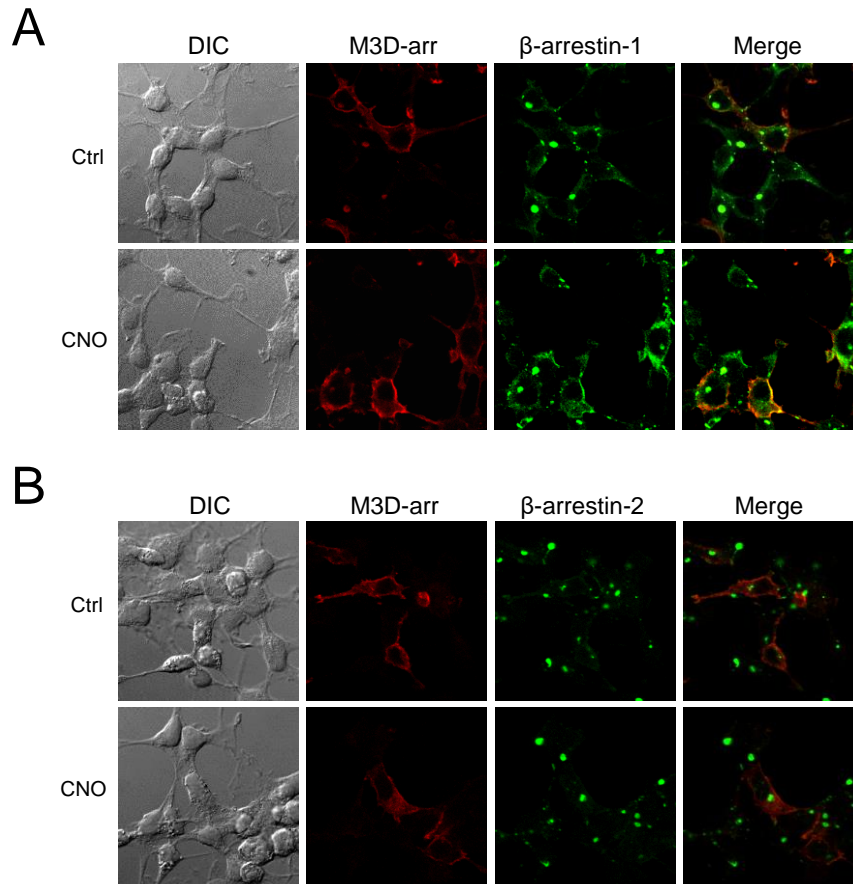


Figure 10. CNO-mediated M3D-arr activation enhances the β -arrestin-1-M3D-arr interaction at the plasma membrane.

Confocal images showing that CNO-treatment intensifies the interaction between β -arrestin-1 and M3D-arr (A), but not the interaction between β -arrestin-2 and M3D-arr (B), at the plasma membrane. M3D-arr-transfected hERG-HEK cells grown on glass coverslips were cultured without (Ctrl) or with 10 μ M CNO for 24 h. M3D-arr was labeled with a rabbit anti-HA primary antibody and an Alexa Fluor 594-conjugated donkey anti-rabbit secondary antibody. β -arrestin-1 or β -arrestin-2 were labelled with goat anti- β -arrestin-1 or mouse anti- β -arrestin-2 primary antibodies and Alexa Fluor 488-conjugated donkey anti-goat or goat anti-mouse secondary antibodies, respectively.

(Wang *et al.*, 2014). As previously mentioned, M3D-arr contains a point mutation (R165L) that disrupts G_q protein-coupling, which should also prevent PKC activation (Nakajima & Wess, 2012). To verify that M3D-arr activation increases mature hERG expression through a PKC-independent pathway, M3D-arr-transfected hERG-HEK cells were cultured without (control) or with CNO in the absence or presence of the PKC inhibitor, H7 (50 μM). Increased mature hERG expression due to CNO-mediated activation of M3D-arr was still present with PKC inhibition (Figure 11A), indicating that alternate pathways are involved.

In addition to G_q proteins, stimulation of muscarinic M3 receptors promotes the activation of phosphoinositide 3-kinase (PI3K) and Akt (Guizzetti & Costa, 2001). Interestingly, β-arrestin-1 has been shown to mediate PI3K/Akt signaling following activation of the insulin-like growth factor-1 receptor (IGF1-R) (Povsic *et al.*, 2003). It has also been reported that PI3K-dependent activation of Akt increases hERG channel function in HEK293 cells (Zhang *et al.*, 2003). Thus, M3D-arr activation and subsequent recruitment of β-arrestin-1 may enhance Akt activation, leading to increased mature hERG expression. To assess whether M3D-arr activation increases mature hERG expression in an Akt-dependent manner, M3D-arr-transfected hERG-HEK cells were cultured without (control) or with CNO in the absence or presence of an Akt1/2 kinase inhibitor (2.5 μM). Inhibition of Akt abolished the CNO-induced increase in mature hERG expression (Figure 11B).

To determine whether CNO-mediated activation of M3D-arr increases Akt activity, we assessed total (non-phosphorylated and phosphorylated) Akt, and active (phosphorylated) Akt expression in M3D-arr-transfected hERG-HEK cells treated with CNO. As shown in Figure 12A, CNO-mediated activation of M3D-arr significantly increased the expression level of active Akt

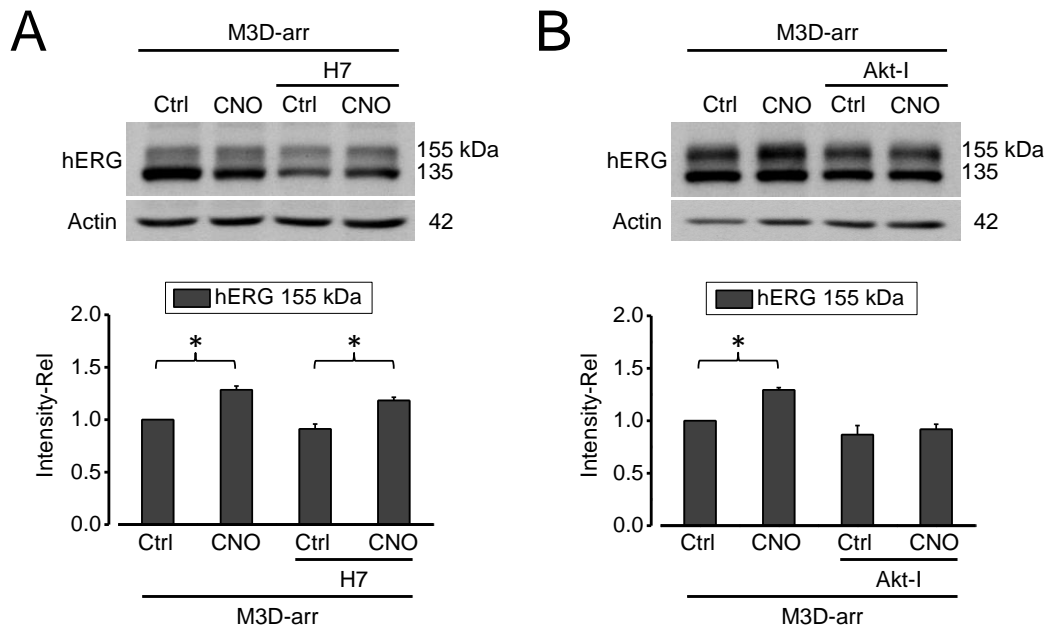


Figure 11. CNO-mediated M3D-arr activation increases hERG expression through an Akt-dependent pathway.

A, PKC inhibition did not affect the M3D-arr activation-induced increase in hERG expression. M3D-arr-transfected hERG-HEK cells were cultured without (Ctrl) or with 10 μ M CNO for 24 hours in the absence or presence of 50 μ M of H7, a PKC inhibitor (n = 3). B, Akt inhibition abolished the M3D-arr activation-induced increase in hERG expression. M3D-arr-transfected hERG-HEK cells were cultured without (Ctrl) or with 10 μ M CNO for 24 hours in the absence or presence of 2.5 μ M of Akt-I, an Akt inhibitor (n = 3). Whole-cell lysates were extracted and assessed using Western Blot analysis. Band intensities of mature (155 kDa) hERG were normalized to respective actin controls and expressed as a value relative to experimental controls in each gel. Data are summarized in the graphs beneath the Western blot images. * $P < 0.05$ vs. Ctrl.

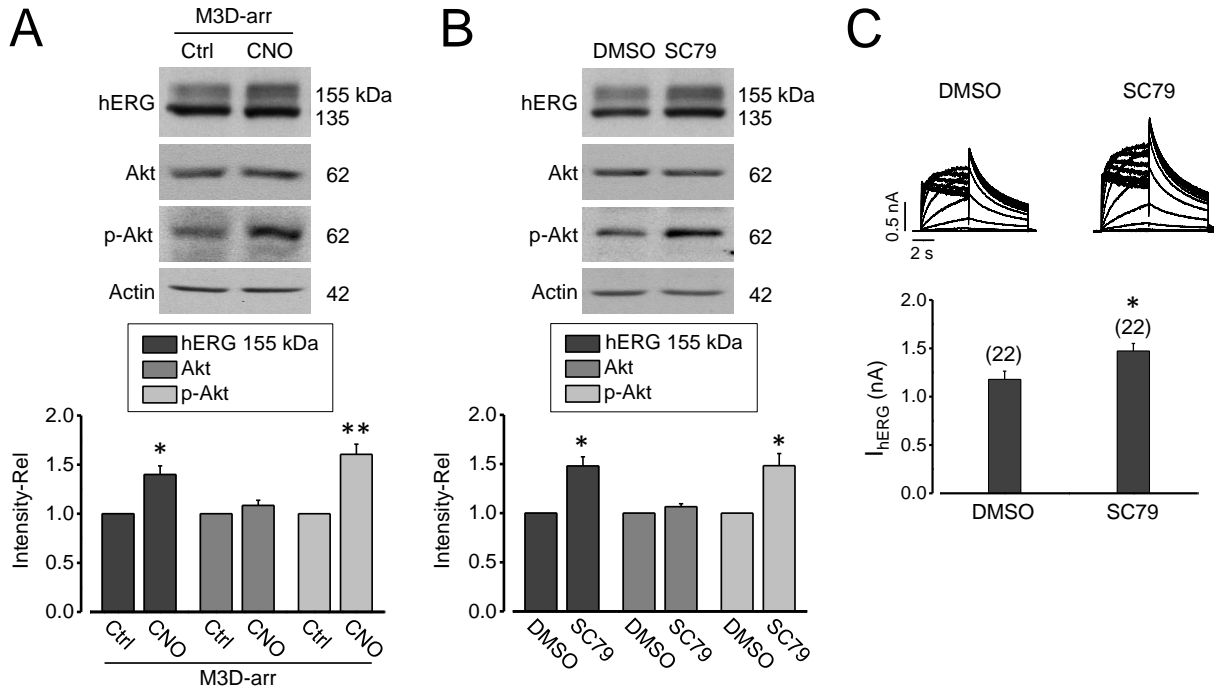


Figure 12. CNO-mediated M3D-arr activation increases the expression level of hERG as well as phosphorylated Akt (p-Akt).

A, Effect of M3D-arr activation on hERG, Akt and p-Akt in M3D-arr-transfected cells cultured without (Ctrl) or with 10 μ M CNO for 24 hours (n = 3). B, Effect of Akt activator, SC79, on hERG, Akt, and p-Akt expression in hERG-HEK cells treated with DMSO (Ctrl) or 12 μ M SC79 for 1 hour (n = 3). Whole-cell lysates were extracted and assessed using Western Blot analysis. Band intensities of mature (155 kDa) hERG, Akt, and p-Akt in CNO- and SC79-treatment groups were normalized to respective actin controls and expressed as a value relative to experimental controls in each gel. Data are summarized in the graphs below the Western blots. C, Effect of SC79 on I_{hERG} . Summarized I_{hERG} is shown beneath the representative families of I_{hERG} from cells treated with DMSO (Ctrl) or SC79. The numbers above the bars indicate the number of cells examined from 3 independent experiments. * $P < 0.05$ or ** $P < 0.01$ vs. Ctrl.

in conjunction with mature hERG protein, but not total Akt. To further demonstrate the effect of Akt activation on mature hERG expression, hERG-HEK cells were cultured with the Akt activator, SC79 (12 μ M). Similar to CNO-mediated activation of M3D-arr, SC79 significantly increased the expression level of active Akt and mature hERG protein (Figure 12B). Concomitantly, treatment with SC79 significantly increased I_{hERG} (Figure 12C).

In addition to pharmacological approaches, we employed molecular biology techniques to characterize the mechanism of Akt activation upon M3D-arr stimulation by CNO. As a phospholipid kinase, PI3K phosphorylates PtdIns(4,5)P₂ to produce PtdIns(3,4,5)P₃ at the plasma membrane (Stephens *et al.*, 1993). Generation of PtdIns(3,4,5)P₃ promotes membrane localization and activation of downstream effectors containing a pleckstrin homology (PH) domain (McManus *et al.*, 2004). In this paradigm, recruitment of phosphoinositide-dependent kinase-1 (PDK1) leads to selective activation of other PH domain-containing kinases such as Akt (Alessi *et al.*, 1997; Bellacosa *et al.*, 1998). It has been well established that PI3K-dependent activation of Akt is antagonized by PTEN (phosphatase and tensin homolog deleted on chromosome 10), which opposes the production of PtdIns(3,4,5)P₃ (Maehama & Dixon, 1998). Thus, we overexpressed PTEN in M3D-arr-transfected hERG-HEK cells and examined the effect of CNO treatment on active Akt and mature hERG expression. Western blot analysis showed that overexpression of PTEN abolished the CNO-induced increase in active Akt and mature hERG expression (Figure 13A). These data are supported by whole-cell patch clamp recordings which showed that constitutively active PTEN eliminated the CNO-induced increase in I_{hERG} (Figure 13B).

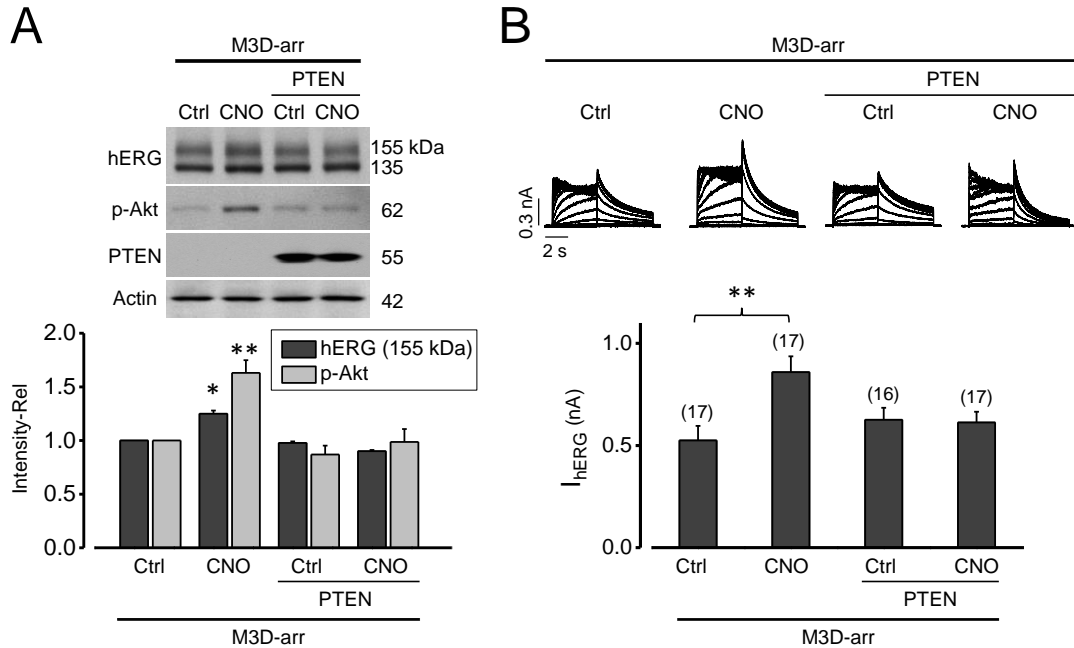


Figure 13. CNO-mediated M3D-arr activation increases mature hERG expression and I_{hERG} through PI3K-mediated activation of Akt.

M3D-arr-transfected hERG-HEK cells were additionally transfected without or with the PI3K inhibitor, PTEN. Cells were then cultured without (Ctrl) or with 10 μ M CNO for 24 h. **A**, The PI3K inhibitor, PTEN, blocked the CNO-induced increase in mature hERG and p-Akt expression. Whole-cell lysates were extracted and assessed using Western Blot analysis. Band intensities of mature (155 kDa) hERG and p-Akt in CNO-treatment groups were normalized to respective actin controls and expressed as a value relative to experimental controls in each gel. Data were summarized in the graph below the Western blot images (n = 3). **B**, The PI3K inhibitor, PTEN, blocked the CNO-induced increase in I_{hERG} . Summarized I_{hERG} is shown beneath the representative families of I_{hERG} in each condition. The numbers above the bars indicate the number of cells examined from 3 independent experiments. * $P < 0.05$ or ** $P < 0.01$ vs. Ctrl.

3.4 Inhibition of PIKfyve or Rab11 abolishes the effect of CNO-mediated M3D-arr activation on I_{hERG} .

A downstream target of Akt, phosphatidylinositol 3-phosphate 5-kinase (PIKfyve), has been demonstrated to promote endosomal trafficking of Kv7.1 channels and GLUT4 carriers to the cell surface (Berwick *et al.*, 2004; Seebohm *et al.*, 2007). Upon phosphorylation by Akt, PIKfyve phosphorylates PtdIns(3)P to produce PtdIns(3,5)P₂, a phospholipid implicated in the stability of intracellular vesicles (Berwick *et al.*, 2004). Therefore, we hypothesized that CNO-mediated activation of M3D-arr increases I_{hERG} through Akt-dependent activation of PIKfyve. To evaluate the role of PIKfyve in this pathway, hERG-HEK cells were transfected with M3D-arr and cultured without (control) or with CNO, in the absence or presence of the PIKfyve inhibitor, YM201636 for 24 h. Inhibition of PIKfyve abolished the CNO-induced increase in I_{hERG} (Figure 14).

We previously demonstrated that the small GTPase Rab11 is involved in the recycling of hERG channels (Chen *et al.*, 2015). Furthermore, we showed that SGK1 and SGK3 enhance hERG expression partially through promoting Rab11-mediated channel recycling (Lamothe & Zhang, 2013). It was also reported that SGK phosphorylates and stimulates PIKfyve, which enhances PtdIns(3,5)P₂ levels in endosomal vesicles, to promote Rab11-mediated insertion of Kv7.1 channels to the membrane (Seebohm *et al.*, 2007). Therefore, we hypothesized that CNO-mediated activation of M3D-arr enhances I_{hERG} through Akt-dependent activation of PIKfyve, which in turn promotes Rab11-mediated recycling of channels to the plasma membrane. To test this hypothesis, we interfered with Rab11 function by overexpressing a Rab11 dominant-negative (DN) mutant in M3D-arr-transfected hERG-HEK cells and examined the effect of CNO on I_{hERG} . As we demonstrated previously, overexpression of Rab11 DN reduced I_{hERG} in control

cells due to the fact that Rab11 plays a role in hERG homeostasis. Furthermore, overexpression of Rab11 DN abolished the CNO-induced increase in I_{hERG} (Figure 14).

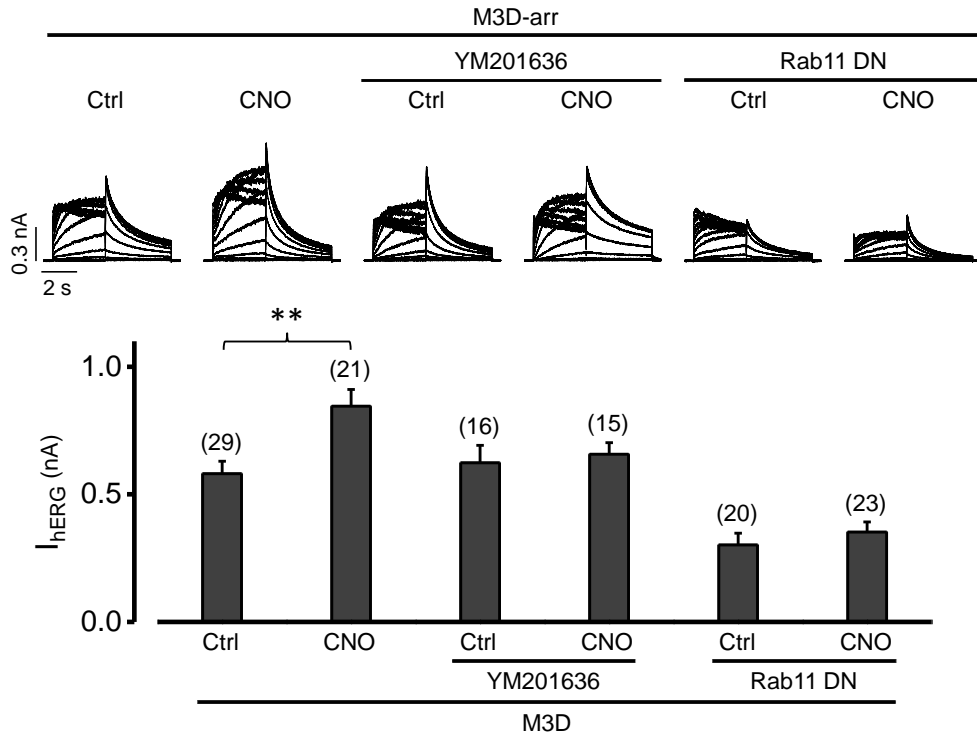


Figure 14. The effect of CNO-mediated M3D-arr activation on I_{hERG} is abolished by inhibition of PIKfyve or Rab11.

Effect of PIKfyve inhibitor, YM201636, as well as overexpression of a Rab11 dominant negative (DN) mutant S25N on I_{hERG} in the absence or presence of CNO-mediated M3D-arr activation. To assess the effects of PIKfyve inhibition, M3D-arr-transfected hERG-HEK cells were cultured without (Ctrl) or with CNO (10 μ M, 24 hours), in the absence or presence of the PIKfyve inhibitor, YM201636 (0.2 μ M). To assess the effects of Rab11 inhibition, M3D-arr-transfected hERG-HEK cells were additionally transfected without or with the Rab11 DN plasmid. Cells were then cultured without (Ctrl) or with of 10 μ M CNO for 24 h. Summarized I_{hERG} is shown beneath the representative families of I_{hERG} in each condition. The numbers above the bars indicate the number of cells examined from 3 independent experiments. $**P < 0.01$ vs. Ctrl.

Chapter 4: Discussion

The voltage-gated K^+ channel, hERG, which passes the rapidly activating delayed rectifier K^+ current (I_{Kr}), is important for the repolarization of cardiomyocyte action potentials (Sanguinetti *et al.*, 1995). Loss-of-function mutations or pharmacological blockage can reduce hERG function, leading to the onset of LQTS. Many LQT2-associated missense mutations reduce hERG current through retention of trafficking-deficient, yet functional channels in the ER (Anderson *et al.*, 2006). Therefore, elucidating the regulation of hERG trafficking is of biological and clinical importance. Indeed, some trafficking-deficient hERG mutants express current after rescue by incubation in low temperature or application of pharmacological chaperones such as E-4031 (Zhou *et al.*, 1999; Anderson *et al.*, 2006). Although effective *in vitro*, these interventions have limited clinical utility *in vivo*, due to the fact that low temperatures are not viable and most rescue reagents block hERG channel conduction.

We recently identified the role of muscarinic receptors in hERG regulation, showing that M3 receptor activation enhances hERG channel expression by inhibiting the E3 ubiquitin ligase Nedd4-2 through G_q protein-dependent activation of PKC (Wang *et al.*, 2014). Upon activation, M3 receptors also recruit β -arrestins to scaffold G_q protein-independent signaling (Novi *et al.*, 2005). However, the role of β -arrestin signaling in hERG regulation has not been previously studied.

The arrestin-biased M3 designer-receptor exclusively activated by CNO (M3D-arr) provides a powerful means for the investigation of β -arrestin signaling in the absence of G_q protein activity (Nakajima & Wess, 2012). Since the M3D-arr construct has never been used in the study of hERG channels, concentration- and time-dependent CNO treatments were employed

to determine the optimal effect on hERG expression (Figure 6A and B). These data validate the lack of M3D-arr constitutive activity and the exclusive affinity of CNO for M3D-arr over endogenous M3 receptors in hERG-HEK cells. Furthermore, our data show that CNO-mediated activation of M3D-arr significantly increased expression of mature hERG protein (155 kDa), but not immature hERG protein (135 kDa) in hERG-HEK cells (Figure 7A). These findings suggest that there is no augmentation of channel biosynthesis. We further validated this notion by analyzing relative hERG mRNA levels, which were unaffected by CNO-mediated activation of M3D-arr (Figure 7B). Functional hERG channels are comprised of mature hERG proteins, which are formed through the glycosylation of immature hERG proteins. Here we show that CNO-mediated activation of M3D-arr selectively increases mature hERG expression without increasing relative hERG mRNA levels. Therefore, the observed increase in mature hERG expression is not due to enhanced channel biosynthesis. It is well understood that the cell surface density of hERG channels is a key determinant of channel function. Here we demonstrated that CNO-mediated activation of M3D-arr significantly increased I_{hERG} , whereas CNO treatment in the absence of M3D-arr had no effect (Figure 8A). We further assessed the effect of CNO on hERG gating kinetics, showing that CNO treatment did not significantly alter the half activation voltage or slope of the activation curve in both pcDNA3- and M3D-arr-transfected hERG-HEK cells (Figure 8B). For the first time, these data characterize the effect of CNO on hERG current and kinetics. This represents an important finding in the study of hERG channels, as most drugs block channel conductance (Sanguinetti & Tristani-Firouzi, 2006). Therefore, CNO-mediated activation of M3D-arr likely increases I_{hERG} solely through increased cell surface expression of hERG channels.

Upon ligand-binding, G protein-coupled receptor kinases (GRKs) phosphorylate serine/threonine residues in the third intracellular loop and C-terminus of GPCRs to promote β -arrestin recruitment (Oakley *et al.*, 2001; Reiter & Lefkowitz, 2006). In the context of M3 receptors, stimulation by carbachol promotes the recruitment and interaction with β -arrestin-1 (Novi *et al.*, 2005). Similar to its endogenous M3 receptor counterpart, M3D-arr selectively interacts with β -arrestin-1, but not β -arrestin-2, following stimulation by CNO (Figure 9). We further demonstrated that M3D-arr and β -arrestin-1 spatially overlap at or near the plasma membrane (Figure 10A and B), indicating β -arrestin-1 is recruited to stimulated M3D-arr receptors.

M3D-arr contains a point mutation (R165L) that uncouples G_q protein interactions, allowing for exclusive recruitment of β -arrestin. As a result, M3D-arr loses the capacity to evoke PKC signaling in a G_q protein-dependent fashion. Indeed, we demonstrated that PKC inhibition by H7 did not abolish the CNO-induced increase in mature hERG expression, confirming the absence of PKC signaling (Figure 11A). Our lab has previously shown that carbachol-mediated activation of M3 receptors increases mature hERG expression and I_{hERG} in hERG-HEK cells (Wang *et al.*, 2014). Interestingly, PKC inhibition by H7 effectively blocked the carbachol-induced increase in mature hERG expression. This discrepant effect of PKC inhibition is likely due to a temporal difference between β -arrestin and G_q protein signaling, following receptor activation. As shown in Fig. 1, the CNO-induced increase in mature hERG expression displayed a slow-onset response that peaked at 24 h. However, the carbachol-induced increase in mature hERG expression displayed a fast-onset response that peaked at 8 h (Wang *et al.*, 2014). Since we focused on an 8 h carbachol treatment in the previous study, the G protein-dependent, PKC pathway was observed while the G-protein-independent, β -arrestin pathway had not yet

developed. In fact, we observed that H7 blocked the carbachol-induced increase in mature hERG expression following an 8 h treatment, but not a 24 h treatment (data not shown). The different time courses of action for these two signaling pathways are consistent with the notion that these two pathways function independently (Ahn *et al.*, 2004; Shenoy *et al.*, 2006). A similar phenomenon has been identified with ERK1/2 activation following AT₁R stimulation. β -arrestin-mediated ERK1/2 activation is slow and persistent, whereas G protein-mediated activation is rapid and transient (Ahn *et al.*, 2004). Thus, we conclude that M3 receptor stimulation increases mature hERG expression through temporally distinct signaling mechanisms: an early G_q protein-dependent pathway and a late β -arrestin-dependent pathway.

To elucidate the M3D-arr-mediated β -arrestin signaling pathway, we evaluated the role of Akt. Inhibition of Akt effectively abolished the CNO-induced increase in mature hERG expression (Figure 11B). We measured expression levels of total (non-phosphorylated and phosphorylated) and active (phosphorylated) Akt following M3D-arr activation. Our data show an increase in active Akt expression that parallels an increase in mature hERG expression following CNO treatment (Figure 12A). Furthermore, activation of Akt by the small-molecule activator, SC79, increased mature hERG expression to a similar degree as CNO-mediated activation of M3D-arr (Figure 12B). The increase in mature hERG expression corresponded with an increase in I_{hERG} (Figure 12C). Together, these data suggest Akt is primarily responsible for the observed increase in hERG expression following M3D-arr activation.

Akt is modulated through a variety of upstream regulators. Of notable interest is PI3K, a well-known activator of Akt that is constitutively expressed in the heart and vasculature (Schlüter *et al.*, 1999; Crackower *et al.*, 2002). PI3K phosphorylates PtdIns(4,5)P₂ to produce PtdIns(3,4,5)P₃, which recruits and co-localizes PDK1 with Akt at the plasma membrane by

binding to a common PH domain (Bellacosa *et al.*, 1998). PDK1 subsequently phosphorylates Akt at threonine-308, initiating the activation of Akt (Alessi *et al.*, 1997). The activity of PI3K is antagonized by the lipid phosphatase, PTEN, which opposes production of PtdIns(3,4,5)P₃ (Maehama & Dixon, 1998). Our data showed that PI3K inhibition by PTEN overexpression completely abolished the CNO-induced increase of both mature hERG and active Akt expression in M3D-arr-transfected hERG-HEK cells (Figure 13A). This finding suggests that M3D-arr stimulation enhances Akt activity primarily through a PI3K-dependent mechanism. Basal Akt activation has been previously implicated in maintaining normal hERG channel function (Zhang *et al.*, 2003). Our data demonstrate that β -arrestin signaling, in response to M3D-arr activation, enhances hERG expression and current through PI3K-dependent activation of Akt. The activity of PI3K is regulated by tyrosine phosphorylation of its regulatory subunit, which relieves inhibition of its catalytic domain (Cuevas *et al.*, 2001). The mechanism through which PI3K is activated in our model remains to be elucidated, although β -arrestin is known to scaffold non-receptor tyrosine kinases that may be involved (DeWire *et al.*, 2007).

Akt-mediated activation of PIKfyve has been shown to increase hERG current, although through an unknown mechanism (Pakladok *et al.*, 2013). Our data are consistent with this notion, showing that PIKfyve inhibition attenuates the effect of CNO-mediated activation of M3D-arr on I_{hERG} (Figure 14). Combined with previous findings in this study, these results suggest PIKfyve increases hERG current by enhancing expression in the plasma membrane.

Our lab recently found that Rab11 maintains homeostatic levels of mature hERG channels at the cell surface by facilitating slow endosomal recycling (Chen *et al.*, 2015). Furthermore, Rab11-mediated recycling of hERG channels is enhanced by SGK1 and SGK3, close relatives of Akt (Lamothe & Zhang, 2013). Interestingly, PIKfyve is known to increase PtdIns(3,5)P₂ levels

within endosomal membranes, a phospholipid implicated in the stability of trafficking vesicles (Berwick *et al.*, 2004; Seebohm *et al.*, 2007). More specifically, PtdIns(3,5)P₂ positively regulates Rab11-containing endosomes that traffic Kv7.1 channels to the plasma membrane (Seebohm *et al.*, 2007). Here we show that M3D-arr activation increases hERG expression and function in a similar manner. This notion is supported by the overexpression of Rab11 DN in M3D-arr cells treated with CNO, which abolished the effect of CNO-induced increase in I_{hERG} (Figure 14). Rab11 DN also decreased endogenous I_{hERG}, confirming our previous conclusion that Rab11 plays a role in maintaining homeostatic levels of hERG in the plasma membrane. (Figure 14). Thus, we conclude that CNO-mediated activation of M3D-arr likely promotes Akt-mediated activation of PIKfyve, which promotes Rab11-dependent trafficking of hERG channels.

In summary, using the hERG-HEK system and an arrestin-biased M3 designer receptor exclusively activated by CNO, we demonstrated a novel mechanism of β -arrestin-dependent regulation of hERG channels (Figure 15). CNO-mediated activation of M3D-arr leads to the recruitment of β -arrestin-1, which in turn promotes PI3K-dependent activation of Akt. Enhancement of Akt activity stimulates PIKfyve, which promotes Rab11-mediated hERG recycling, leading to increased mature hERG expression and current (Figure 15). These findings provide novel insight into hERG regulation, which is useful for understanding impaired hERG function and identifying therapeutic targets in the treatment of LQTS.

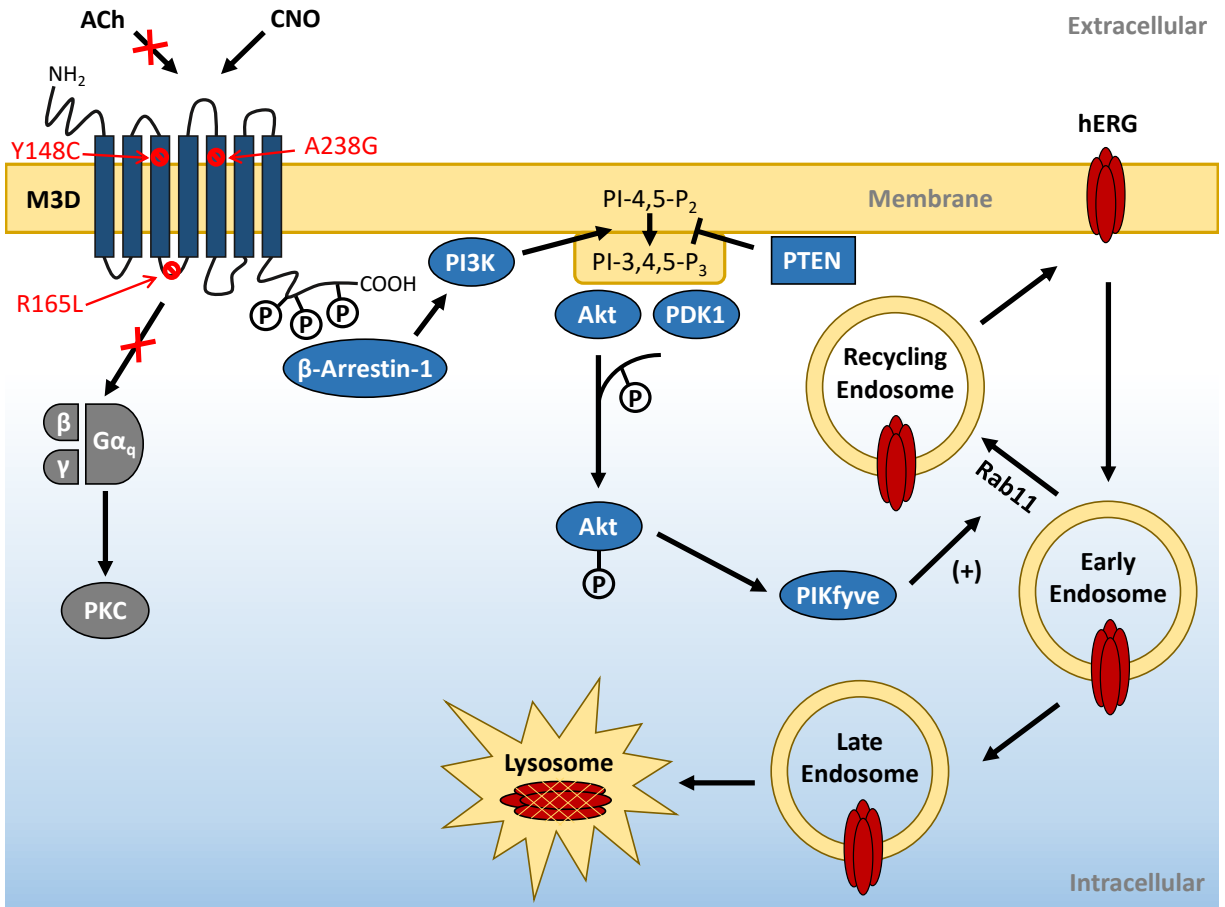


Figure 15. Illustration of M3D-arr-mediated β -arrestin signaling in hERG regulation.

Activation of M3D-arr by CNO leads to the recruitment of β -arrestin-1, which promotes PI3K-dependent activation of Akt. Enhancement of Akt activity stimulates PIKfyve which promotes Rab11-mediated hERG recycling, leading to an increased mature hERG expression.

Future Directions

Further investigation of this work would entail a more extensive dissection of the mechanisms involved in the upregulation of hERG expression. It would be interesting to study which GRK isoforms are involved in the phosphorylation of M3D-arr, which leads to recruitment of β -arrestin-1. Moreover, GPCR interactions with β -arrestin has led to the classification of two types of receptors: Class A receptors, which form a weak, transient interaction with β -arrestin and undergo rapid recycling to the plasma membrane following dissociation; Class B receptors, which form a strong, prolonged interaction with β -arrestin and undergo slow recycling as a complex before trafficking to the membrane. Classifying M3D-arr may provide greater insight into the time-course of β -arrestin signaling and the efficacy of CNO throughout particular treatments.

In the present work, β -arrestin promotes PI3K activity through an unknown mechanism. Activation of PI3K is regulated by tyrosine phosphorylation of its regulatory subunit. Since β -arrestin is known to scaffold non-receptor tyrosine kinases, it may be beneficial to screen for potential candidates that phosphorylate PI3K.

The expression system used in this work is an immortal HEK293 cell line. To examine more physiologically relevant effects of M3D-arr on hERG, a primary cardiomyocyte cell line could be employed. Our lab typically utilizes neonatal rat cardiomyocytes for such experiments.

Although beyond the scope of the current work, implementing M3D-arr in transgenic animal models would provide a means of studying the *in vivo* effects of β -arrestin signaling on cardiac electrophysiology. This could be accomplished with heart-specific expression of M3D-arr combined with intravenous administration of CNO.

References

- Ahn S, Shenoy SK, Wei H & Lefkowitz RJ (2004). Differential kinetic and spatial patterns of β -arrestin and G protein-mediated ERK activation by the angiotensin II receptor. *J Biol Chem* **279**, 35518–35525.
- Alessi DR, Andjelkovic M, Caudwell B, Cron P, Morrice N, Cohen P & Hemmings BA (1996). Mechanism of activation of protein kinase B by insulin and IGF-1. *EMBO J* **15**, 6541–6551.
- Alessi DR, James SR, Downes CP, Holmes AB, Gaffney PRJ, Reese CB & Cohen P (1997). Characterization of a 3-phosphoinositide-dependent protein kinase which phosphorylates and activates protein kinase Balpha. *Curr Biol* **7**, 261–269.
- Alexandrov K, Horiuchi H, Steele-Mortimer O, Seabra MC & Zerial M (1994). Rab escort protein-1 is a multifunctional protein that accompanies newly prenylated rab proteins to their target membranes. *EMBO J* **13**, 5262–5273.
- Alvarez-Curto E, Prihandoko R, Tautermann CS, Zwier JM, Padiani JD, Lohse MJ, Hoffmann C, Tobin AB & Milligan G (2011). Developing chemical genetic approaches to explore G protein-coupled receptor function: validation of the use of a receptor activated solely by synthetic ligand (RASSL). *Mol Pharmacol* **80**, 1033–1046.
- Ambrose C, James M, Barnes G, Lin C, Bates G, Altherr M, Duyao M, Groot N, Church D & Wasmuth JJ (1992). A novel G protein-coupled receptor kinase gene cloned from 4p16.3. *Hum Mol Genet* **1**, 697–703.
- Anderson CL, Delisle BP, Anson BD, Kilby JA, Will ML, Tester DJ, Gong Q, Zhou Z, Ackerman MJ & January CT (2006). Most LQT2 mutations reduce Kv11.1 (hERG) current by a class 2 (trafficking-deficient) mechanism. *Circulation* **113**, 365–373.
- Armbruster BN, Li X, Pausch MH, Herlitz S & Roth BL (2007). Evolving the lock to fit the key to create a family of G protein-coupled receptors potently activated by an inert ligand. *Proc Natl Acad Sci U S A* **104**, 5163–5168.
- Attramadal H, Arriza JL, Aoki C, Dawson TM, Codina J, Kwatra MM, Snyder SH, Caron MG & Lefkowitz RJ (1992). Beta-arrestin2, a novel member of the arrestin/beta-arrestin gene family. *J Biol Chem* **267**, 17882–17890.
- Bellacosa A, Chan TO, Ahmed NN, Datta K, Malstrom S, Stokoe D, McCormick F, Feng J & Tsichlis P (1998). Akt activation by growth factors is a multiple-step process: the role of the PH domain. *Oncogene* **17**, 313–325.
- Benovic JL & Gomez J (1993). Molecular cloning and expression of GRK6. A new member of the G

- protein-coupled receptor kinase family. *J Biol Chem* **268**, 19521–19527.
- Benovic JL, Strasser RH, Caron MG & Lefkowitz RJ (1986). Beta-adrenergic receptor kinase: identification of a novel protein kinase that phosphorylates the agonist-occupied form of the receptor. *Proc Natl Acad Sci U S A* **83**, 2797–2801.
- Berwick DC, Dell GC, Welsh GI, Heesom KJ, Hers I, Fletcher LM, Cooke FT & Tavaré JM (2004). Protein kinase B phosphorylation of PIKfyve regulates the trafficking of GLUT4 vesicles. *J Cell Sci* **117**, 5985–5993.
- Biondi RM, Kieloch A, Currie RA, Deak M & Alessi DR (2001). The PIF-binding pocket in PDK1 is essential for activation of S6K and SGK, but not PKB. *EMBO J* **20**, 4380–4390.
- Brink CB, Harvey BH, Bodenstein J, Venter DP & Oliver DW (2004). Recent advances in drug action and therapeutics: Relevance of novel concepts in G-protein-coupled receptor and signal transduction pharmacology. *Br J Clin Pharmacol* **57**, 373–387. Available at: <http://www.ncbi.nlm.nih.gov/pubmed/15025734> [Accessed August 2, 2016].
- Brock C, Schaefer M, Reusch HP, Czupalla C, Michalke M, Spicher K, Schultz G & Nürnberg B (2003). Roles of G beta gamma in membrane recruitment and activation of p110 gamma/p101 phosphoinositide 3-kinase gamma. *J Cell Biol* **160**, 89–99.
- Bucci C et al. (1992). The small GTPase rab5 functions as a regulatory factor in the early endocytic pathway. *Cell* **70**, 715–728.
- Burke JE & Williams RL (2013). Dynamic steps in receptor tyrosine kinase mediated activation of class IA phosphoinositide 3-kinases (PI3K) captured by H/D exchange (HDX-MS). *Adv Biol Regul* **53**, 97–110.
- Chen J, Guo J, Yang T, Li W, Lamothe SM, Kang Y, Szendrey JA & Zhang S (2015). Rab11-dependent recycling of the human ether-a-go-gorelated gene (hERG) channel. *J Biol Chem* **290**, 21101–21113.
- Crackower MA et al. (2002). Regulation of myocardial contractility and cell size by distinct PI3K-PTEN signaling pathways. *Cell* **110**, 737–749.
- Cuevas BD, Lu Y, Mao M, Zhang J, LaPushin R, Siminovitch K & Mills GB (2001). Tyrosine phosphorylation of p85 relieves its inhibitory activity on phosphatidylinositol 3-kinase. *J Biol Chem* **276**, 27455–27461.
- Curran ME, Splawski I, Timothy KW, Vincent GM, Green ED & Keating MT (1995). A molecular basis for cardiac arrhythmia: HERG mutations cause long QT syndrome. *Cell* **80**, 795–803.
- Das S, Dixon JE & Cho W (2003). Membrane-binding and activation mechanism of PTEN. *Proc Natl Acad Sci U S A* **100**, 7491–7496.
- Delisle BP, Underkofler HAS, Moungey BM, Slind JK, Kilby JA, Best JM, Foell JD, Balijepalli RC, Kamp TJ & January CT (2009). Small GTPase determinants for the golgi processing and

- plasmalemmal expression of human ether-a-go-go related (hERG) K⁺ channels. *J Biol Chem* **284**, 2844–2853.
- DeWire SM, Ahn S, Lefkowitz RJ & Shenoy SK (2007). Beta-arrestins and cell signaling. *Annu Rev Physiol* **69**, 483–510.
- Doherty GJ & McMahon HT (2009). Mechanisms of endocytosis. *Annu Rev Biochem* **78**, 857–902.
- Doyle DA, Morais Cabral J, Pfuetzner RA, Kuo A, Gulbis JM, Cohen SL, Chait BT & MacKinnon R (1998). The structure of the potassium channel: molecular basis of K⁺ conduction and selectivity. *Science* **280**, 69–77.
- Eglen RM (2012). Overview of muscarinic receptor subtypes. *Handb Exp Pharmacol* 3–28.
- Ferrer T, Rupp J, Piper DR & Tristani-Firouzi M (2006). The S4-S5 linker directly couples voltage sensor movement to the activation gate in the human ether-a'-go-go-related gene (hERG) K⁺ channel. *J Biol Chem* **281**, 12858–12864.
- Ficker E, Dennis AT, Wang L & Brown AM (2003). Role of the cytosolic chaperones Hsp70 and Hsp90 in maturation of the cardiac potassium channel HERG. *Circ Res* **92**, e87–e100.
- Ficker E, Obejero-Paz CA, Zhao S & Brown AM (2002). The binding site for channel blockers that rescue misprocessed human long QT syndrome type 2 ether-a-gogo-related gene (HERG) mutations. *J Biol Chem* **277**, 4989–4998.
- Foster FM, Traer CJ, Abraham SM & Fry MJ (2003). The phosphoinositide (PI) 3-kinase family. *J Cell Sci* **116**, 3037–3040.
- Gillooly DJ, Morrow IC, Lindsay M, Gould R, Bryant NJ, Gaullier JM, Parton RG & Stenmark H (2000). Localization of phosphatidylinositol 3-phosphate in yeast and mammalian cells. *EMBO J* **19**, 4577–4588.
- Gong Q, Anderson CL, January CT & Zhou Z (2002). Role of glycosylation in cell surface expression and stability of HERG potassium channels. *Am J Physiol - Hear Circ Physiol* **283**, H77–H84.
- Goodman OB, Krupnick JG, Santini F, Gurevich V V, Penn RB, Gagnon AW, Keen JH & Benovic JL (1996). Beta-arrestin acts as a clathrin adaptor in endocytosis of the beta2-adrenergic receptor. *Nature* **383**, 447–450.
- Grant AO (2009). Cardiac ion channels. *Circ Arrhythmia Electrophysiol* **2**, 185–194.
- Grosshans BL, Ortiz D & Novick P (2006). Rabs and their effectors: achieving specificity in membrane traffic. *Proc Natl Acad Sci U S A* **103**, 11821–11827.
- Grunnet M (2010). Repolarization of the cardiac action potential. Does an increase in repolarization capacity constitute a new anti-arrhythmic principle? *Acta Physiol*. Available at: <http://www.ncbi.nlm.nih.gov/pubmed/20132149>.
- Grunnet M, Olesen SP, Klaerke DA & Jespersen T (2005). hKCNE4 inhibits the hKCNQ1 potassium

- current without affecting the activation kinetics. *Biochem Biophys Res Commun* **328**, 1146–1153.
- Guizzetti M & Costa LG (2001). Activation of phosphatidylinositol 3 kinase by muscarinic receptors in astrocytoma cells. *Neuroreport* **12**, 1639–1642.
- Guo D & Lu Z (2000). Mechanism of IRK1 channel block by intracellular polyamines. *J Gen Physiol* **115**, 799–814.
- Guo J, Massaelli H, Xu J, Jia Z, Wigle JT, Mesaelli N & Zhang S (2009). Extracellular K⁺ concentration controls cell surface density of IKr in rabbit hearts and of the HERG channel in human cell lines. *J Clin Invest* **119**, 2745–2757.
- Guo J, Wang T, Li X, Shallow H, Yang T, Li W, Xu J, Fridman MD, Yang X & Zhang S (2012). Cell surface expression of human ether-a-go-go-related gene (hERG) channels is regulated by caveolin-3 protein via the ubiquitin ligase Nedd4-2. *J Biol Chem* **287**, 33132–33141.
- Hanada M, Feng J & Hemmings BA (2004). Structure, regulation and function of PKB/AKT - A major therapeutic target. *Biochim Biophys Acta - Proteins Proteomics* **1697**, 3–16.
- Hansen CG & Nichols BJ (2009). Molecular mechanisms of clathrin-independent endocytosis. *J Cell Sci* **122**, 1713–1721.
- Harvey RD (2012). Muscarinic receptor agonists and antagonists: effects on cardiovascular function. *Handb Exp Pharmacol* 299–316.
- Hermans E (2003). Biochemical and pharmacological control of the multiplicity of coupling at G-protein-coupled receptors. *Pharmacol Ther* **99**, 25–44.
- Hutagalung AH & Novick PJ (2011). Role of Rab GTPases in membrane traffic and cell physiology. *Physiol Rev* **91**, 119–149.
- Kang Y, Guo J, Yang T, Li W & Zhang S (2015). Regulation of the human ether-a-go-go-related gene (hERG) potassium channel by Nedd4 family interacting proteins (Ndfips). *Biochem J* **472**, 71–82.
- Keating MT & Sanguinetti MC (2001). Molecular and cellular mechanisms review of cardiac arrhythmias. *Cell* **104**, 569–580.
- Kunapuli P & Benovic JL (1993). Cloning and expression of GRK5: a member of the G protein-coupled receptor kinase family. *Proc Natl Acad Sci U S A* **90**, 5588–5592.
- Lamothe SM & Zhang S (2013). The serum- and glucocorticoid-inducible kinases SGK1 and SGK3 regulate hERG channel expression via ubiquitin ligase Nedd4-2 and GTPase Rab11. *J Biol Chem* **288**, 15075–15084.
- Lee DK, Nguyen T, Lynch KR, Cheng R, Vanti WB, Arkhitko O, Lewis T, Evans JF, George SR & O'Dowd BF (2001). Discovery and mapping of ten novel G protein-coupled receptor genes. *Gene* **275**, 83–91.
- Lee J-O, Yang H, Georgescu M-M, Di Cristofano A, Maehama T, Shi Y, Dixon JE, Pandolfi P &

- Pavletich NP (1999). Crystal Structure of the PTEN Tumor Suppressor: Implications for Its Phosphoinositide Phosphatase Activity and Membrane Association. *Cell* **99**, 323–334.
- Leslie NR & Downes CP (2002). PTEN: The down side of PI 3-kinase signalling. *Cell Signal* **14**, 285–295.
- von Lewinski D, Voss K, Hülsmann S, Kögler H & Pieske B (2003). Insulin-like growth factor-1 exerts Ca²⁺-dependent positive inotropic effects in failing human myocardium. *Circ Res* **92**, 169–176.
- Liao Y & Hung M-C (2010). Physiological regulation of Akt activity and stability. *Am J Transl Res* **2**, 19–42.
- Liu Y & Sun L (2011). <Title/>. *Mol Med* **17**, 1.
- Lombardi D, Soldati T, Riederer MA, Goda Y, Zerial M & Pfeffer SR (1993). Rab9 functions in transport between late endosomes and the trans Golgi network. *EMBO J* **12**, 677–682.
- Lorenz W, Inglese J, Palczewski K, Onorato JJ, Caron MG & Lefkowitz RJ (1991). The receptor kinase family: primary structure of rhodopsin kinase reveals similarities to the beta-adrenergic receptor kinase. *Proc Natl Acad Sci U S A* **88**, 8715–8719.
- Lu Y, Mahaut-Smith MP, Varghese A, Huang CL, Kemp PR & Vandenberg JI (2001). Effects of premature stimulation on HERG K(+) channels. *J Physiol* **537**, 843–851.
- Maehama T & Dixon JE (1998). The tumor suppressor, PTEN/MMAC1, dephosphorylates the lipid second messenger, phosphatidylinositol 3,4,5-trisphosphate. *J Biol Chem* **273**, 13375–13378.
- Manning BD & Cantley LC (2007). AKT/PKB signaling: navigating downstream. *Cell* **129**, 1261–1274.
- Massaeli H, Sun T, Li X, Shallow H, Wu J, Xu J, Li W, Hanson C, Guo J & Zhang S (2010). Involvement of caveolin in low K⁺-induced endocytic degradation of cell-surface human ether-a-go-go-related gene (hERG) channels. *J Biol Chem* **285**, 27259–27264.
- McManus EJ, Collins BJ, Ashby PR, Prescott AR, Murray-Tait V, Armit LJ, Arthur JSC & Alessi DR (2004). The in vivo role of PtdIns(3,4,5)P₃ binding to PDK1 PH domain defined by knockin mutation. *EMBO J* **23**, 2071–2082.
- Milburn CC, Deak M, Kelly SM, Price NC, Alessi DR & Van Aalten DMF (2003). Binding of phosphatidylinositol 3,4,5-trisphosphate to the pleckstrin homology domain of protein kinase B induces a conformational change. *Biochem J* **375**, 531–538.
- Murga C, Laguine L, Wetzker R, Cuadrado A & Gutkind JS (1998). Activation of Akt/protein kinase B by G protein-coupled receptors. A role for alpha and beta gamma subunits of heterotrimeric G proteins acting through phosphatidylinositol-3-OH kinase gamma. *J Biol Chem* **273**, 19080–19085.
- Nakajima K & Wess J (2012). Design and functional characterization of a novel, arrestin-biased designer G protein-coupled receptor. *Mol Pharmacol* **82**, 575–582.
- Novi F, Stanasila L, Giorgi F, Corsini GU, Cotecchia S & Maggio R (2005). Paired activation of two

- components within muscarinic M3 receptor dimers is required for recruitment of β -arrestin-1 to the plasma membrane. *J Biol Chem* **280**, 19768–19776.
- Oakley RH, Laporte SA, Holt JA, Barak LS & Caron MG (2001). Molecular determinants underlying the formation of stable intracellular G protein-coupled receptor-beta-arrestin complexes after receptor endocytosis*. *J Biol Chem* **276**, 19452–19460.
- Oakley RH, Laporte SA, Holt JA, Caron MG & Barak LS (2000). Differential affinities of visual arrestin, beta arrestin1, and beta arrestin2 for G protein-coupled receptors delineate two major classes of receptors. *J Biol Chem* **275**, 17201–17210.
- Oudit GY & Penninger JM (2009). Cardiac regulation by phosphoinositide 3-kinases and PTEN. *Cardiovasc Res* **82**, 250–260.
- Pakladok T, Almilaji A, Munoz C, Alesutan I & Lang F (2013). PIKfyve sensitivity of hERG channels. *Cell Physiol Biochem* **31**, 785–794.
- Pals-Rylaarsdam R, Gurevich V V, Lee KB, Ptasienski JA, Benovic JL & Hosey MM (1997). Internalization of the m2 muscarinic acetylcholine receptor. Arrestin-independent and -dependent pathways. *J Biol Chem* **272**, 23682–23689.
- Parruti G, Ambrosini G, Sallese M & De Blasi A (1993). Molecular cloning, functional expression and mRNA analysis of human beta-adrenergic receptor kinase 2. *Biochem Biophys Res Commun* **190**, 475–481.
- Parton RG & Simons K (2007). The multiple faces of caveolae. *Nat Rev Mol Cell Biol* **8**, 185–194.
- Pereira-Leal JB & Seabra MC (2000). The mammalian Rab family of small GTPases: definition of family and subfamily sequence motifs suggests a mechanism for functional specificity in the Ras superfamily. *J Mol Biol* **301**, 1077–1087.
- Perrin MJ, Subbiah RN, Vandenberg JI & Hill AP (2008). Human ether-a-go-go related gene (hERG) K⁺ channels: Function and dysfunction. *Prog Biophys Mol Biol* **98**, 137–148.
- Pfister C, Chabre M, Plouet J, Tuyen V V, De Kozak Y, Faure JP & Kühn H (1985). Retinal S antigen identified as the 48K protein regulating light-dependent phosphodiesterase in rods. *Science* **228**, 891–893.
- Pierce KL, Premont RT & Lefkowitz RJ (2002). Seven-transmembrane receptors. *Nat Rev Mol Cell Biol* **3**, 639–650.
- Pochynyuk O, Stockand JD & Staruschenko A (2007). Ion channel regulation by Ras, Rho, and Rab small GTPases. *Exp Biol Med (Maywood)* **232**, 1258–1265.
- Povsic TJ, Kohout TA & Lefkowitz RJ (2003). β -Arrestin1 Mediates Insulin-like Growth Factor 1 (IGF-1) Activation of Phosphatidylinositol 3-Kinase (PI3K) and Anti-apoptosis. *J Biol Chem* **278**, 51334–51339.

- Rak A, Pylypenko O, Durek T, Watzke A, Kushnir S, Brunsveld L, Waldmann H, Goody RS & Alexandrov K (2003). Structure of Rab GDP-dissociation inhibitor in complex with prenylated YPT1 GTPase. *Science* **302**, 646–650.
- Reiter E & Lefkowitz RJ (2006). GRKs and β -arrestins: roles in receptor silencing, trafficking and signaling. *Trends Endocrinol Metab* **17**, 159–165. Available at: <http://www.ncbi.nlm.nih.gov/pubmed/16595179> [Accessed August 2, 2016].
- Roseberry AG & Hosey MM (2001). Internalization of the M2 muscarinic acetylcholine receptor proceeds through an atypical pathway in HEK293 cells that is independent of clathrin and caveolae. *J Cell Sci* **114**, 739–746.
- Rothberg KG, Heuser JE, Donzell WC, Ying Y-S, Glenney JR & Anderson RGW (1992). Caveolin, a protein component of caveolae membrane coats. *Cell* **68**, 673–682.
- Sanguinetti MC, Jiang C, Curran ME & Keating MT (1995). A mechanistic link between an inherited and an acquired cardiac arrhythmia: HERG encodes the IKr potassium channel. *Cell* **81**, 299–307.
- Sanguinetti MC & Jurkiewicz NK (1990). Two components of cardiac delayed rectifier K⁺ current. Differential sensitivity to block by class III antiarrhythmic agents. *J Gen Physiol* **96**, 195–215.
- Sanguinetti MC & Tristani-Firouzi M (2006). hERG potassium channels and cardiac arrhythmia. *Nature* **440**, 463–469.
- Sarbassov DD, Guertin DA, Ali SM & Sabatini DM (2005). Phosphorylation and regulation of Akt/PKB by the rictor-mTOR complex. *Science* **307**, 1098–1101.
- Sbrissa D, Ikonomov OC & Shisheva A (1999). PIKfyve, a mammalian ortholog of yeast Fab1p lipid kinase, synthesizes 5-phosphoinositides. Effect of insulin. *J Biol Chem* **274**, 21589–21597.
- Sbrissa D, Ikonomov OC & Shisheva A (2002). Phosphatidylinositol 3-phosphate-interacting domains in PIKfyve. Binding specificity and role in PIKfyve. Endomembrane localization. *J Biol Chem* **277**, 6073–6079.
- Scherer PE, Okamoto T, Chun M, Nishimoto I, Lodish HF & Lisanti MP (1996). Identification, sequence, and expression of caveolin-2 defines a caveolin gene family. *Proc Natl Acad Sci U S A* **93**, 131–135.
- Schlüter KD, Simm A, Schäfer M, Taimor G & Piper HM (1999). Early response kinase and PI 3-kinase activation in adult cardiomyocytes and their role in hypertrophy. *Am J Physiol* **276**, H1655–H1663.
- Schultz J, Doerks T, Ponting CP, Copley RR & Bork P (2000). More than 1,000 putative new human signalling proteins revealed by EST data mining. *Nat Genet* **25**, 201–204.
- Seeböhm G, Strutz-Seeböhm N, Birkin R, Dell G, Bucci C, Spinosa MR, Baltaev R, Mack AF, Korniychuk G, Choudhury A, Marks D, Pagano RE, Attali B, Pfeufer A, Kass RS, Sanguinetti MC, Tavaré JM & Lang F (2007). Regulation of endocytic recycling of KCNQ1/KCNE1 potassium channels. *Circ Res* **100**, 686–692.

- Shenoy SK, Drake MT, Nelson CD, Houtz DA, Xiao K, Madabushi S, Reiter E, Premont RT, Lichtarge O & Lefkowitz RJ (2006). β -arrestin-dependent, G protein-independent ERK1/2 activation by the β_2 adrenergic receptor. *J Biol Chem* **281**, 1261–1273.
- Shioi T, Kang PM, Douglas PS, Hampe J, Yballe CM, Lawitts J, Cantley LC & Izumo S (2000). The conserved phosphoinositide 3-kinase pathway determines heart size in mice. *EMBO J* **19**, 2537–2548.
- Sivars U, Aivazian D & Pfeffer SR (2003). Yip3 catalyses the dissociation of endosomal Rab-GDI complexes. *Nature* **425**, 856–859.
- van der Sluijs P et al. (1992). The small GTP-binding protein rab4 controls an early sorting event on the endocytic pathway. *Cell* **70**, 729–740.
- Smith PL, Baukowitz T & Yellen G (1996). The inward rectification mechanism of the HERG cardiac potassium channel. *Nature* **379**, 833–836.
- Smith PL & Yellen G (2002). Fast and slow voltage sensor movements in HERG potassium channels. *J Gen Physiol* **119**, 275–293.
- Soldati T, Rancaño C, Geissler H & Pfeffer SR (1995). Rab7 and Rab9 are recruited onto late endosomes by biochemically distinguishable processes. *J Biol Chem* **270**, 25541–25548.
- Sönnichsen B, De Renzis S, Nielsen E, Rietdorf J & Zerial M (2000). Distinct membrane domains on endosomes in the recycling pathway visualized by multicolor imaging of Rab4, Rab5, and Rab11. *J Cell Biol* **149**, 901–914.
- Splawski I, Shen J, Timothy KW, Lehmann MH, Priori S, Robinson JL, Moss a J, Schwartz PJ, Towbin J a, Vincent GM & Keating MT (2000). Spectrum of mutations in long-QT syndrome genes. KVLQT1, HERG, SCN5A, KCNE1, and KCNE2. *Circulation* **102**, 1178–1185.
- Stenmark H (2009). Rab GTPases as coordinators of vesicle traffic. *Nat Rev Mol Cell Biol* **10**, 513–525.
- Stephens LR, Jackson TR & Hawkins PT (1993). Agonist-stimulated synthesis of phosphatidylinositol(3,4,5)-trisphosphate. *Biochim Biophys Acta - Mol Cell Res* **1179**, 27–75.
- Sterne-Marr R, Gurevich V V, Goldsmith P, Bodine RC, Sanders C, Donoso LA & Benovic JL (1993). Polypeptide variants of beta-arrestin and arrestin3. *J Biol Chem* **268**, 15640–15648.
- Sun H, Kerfant B-G, Zhao D, Trivieri MG, Oudit GY, Penninger JM & Backx PH (2006). Insulin-like growth factor-1 and PTEN deletion enhance cardiac L-type Ca²⁺ currents via increased PI3K α /PKB signaling. *Circ Res* **98**, 1390–1397.
- Surawicz B (1989). Electrophysiologic substrate of torsade de pointes: Dispersion of repolarization or early afterdepolarizations? *J Am Coll Cardiol* **14**, 172–184.
- Takeda S, Kadowaki S, Haga T, Takaesu H & Mitaku S (2002). Identification of G protein-coupled receptor genes from the human genome sequence. *FEBS Lett* **520**, 97–101.

- Thiel G, Kaufmann A & Rössler OG (2013). G-protein-coupled designer receptors - new chemical-genetic tools for signal transduction research. *Biol Chem* **394**, 1615–1622.
- Töpert C, Döring F, Wischmeyer E, Karschin C, Brockhaus J, Ballanyi K, Derst C & Karschin A (1998). Kir2.4: a novel K⁺ inward rectifier channel associated with motoneurons of cranial nerve nuclei. *J Neurosci* **18**, 4096–4105.
- Trudeau MC, Warmke JW, Ganetzky B & Robertson GA (1995). HERG, a human inward rectifier in the voltage-gated potassium channel family. *Science (80-)* **269**, 92–95.
- Ugi S, Imamura T, Maegawa H, Egawa K, Yoshizaki T, Shi K, Obata T, Ebina Y, Kashiwagi A & Olefsky JM (2004). Protein phosphatase 2A negatively regulates insulin's metabolic signaling pathway by inhibiting Akt (protein kinase B) activity in 3T3-L1 adipocytes. *Mol Cell Biol* **24**, 8778–8789.
- Ullrich O, Reinsch S, Urbé S, Zerial M & Parton RG (1996). Rab11 regulates recycling through the pericentriolar recycling endosome. *J Cell Biol* **135**, 913–924.
- Vandenberg JJ, Perry MD, Perrin MJ, Mann SA, Ke Y & Hill AP (2012). hERG K⁺ Channels: Structure, Function, and Clinical Significance. *Physiol Rev* **92**, 1393–1478.
- Vanhaesebroeck B, Leever SJ, Ahmadi K, Timms J, Katso R, Driscoll PC, Woscholski R, Parker PJ & Waterfield MD (2001). Synthesis and function of 3-phosphorylated inositol lipids. *Annu Rev Biochem* **70**, 535–602.
- Vanlandingham PA & Ceresa BP (2009). Rab7 regulates late endocytic trafficking downstream of multivesicular body biogenesis and cargo sequestration. *J Biol Chem* **284**, 12110–12124.
- Vincent GM, Timothy KW, Leppert M & Keating M (1992). The spectrum of symptoms and QT intervals in carriers of the gene for the long-QT syndrome. *N Engl J Med* **327**, 846–852.
- Wang Q, Curran ME, Splawski I, Burn TC, Millholland JM, VanRaay TJ, Shen J, Timothy KW, Vincent GM, de Jager T, Schwartz PJ, Toubin JA, Moss AJ, Atkinson DL, Landes GM, Connors TD & Keating MT (1996). Positional cloning of a novel potassium channel gene: KVLQT1 mutations cause cardiac arrhythmias. *Nat Genet* **12**, 17–23.
- Wang Q, Shen J, Splawski I, Atkinson D, Li Z, Robinson JL, Moss AJ, Towbin JA & Keating MT (1995). SCN5A mutations associated with an inherited cardiac arrhythmia, long QT syndrome. *Cell* **80**, 805–811.
- Wang T, Hogan-Cann A, Kang Y, Cui Z, Guo J, Yang T, Lamothe SM, Li W, Ma A, Fisher JT & Zhang S (2014). Muscarinic Receptor Activation Increases Herg Channel Expression through Phosphorylation of Ubiquitin Ligase Nedd4-2. *Mol Pharmacol* **85**, 877–886.
- Wang Y, Huang X, Zhou J, Yang X, Li D, Mao H, Sun HH, Liu N & Lian J (2012). Trafficking-deficient G572R-hERG and E637K-hERG activate stress and clearance pathways in endoplasmic reticulum.

PLoS One **7**, e29885.

- Wei H, Ahn S, Shenoy SK, Karnik SS, Hunyady L, Luttrell LM & Lefkowitz RJ (2003). Independent β -arrestin 2 and G protein-mediated pathways for angiotensin II activation of extracellular signal-regulated kinases 1 and 2. *Proc Natl Acad Sci U S A* **100**, 10782–10787.
- Weiss ER, Raman D, Shirakawa S, Ducceschi MH, Bertram PT, Wong F, Kraft TW & Osawa S (1998). The cloning of GRK7, a candidate cone opsin kinase, from cone- and rod-dominant mammalian retinas. *Mol Vis* **4**, 27.
- Wess J, Nakajima K & Jain S (2013). Novel designer receptors to probe GPCR signaling and physiology. *Trends Pharmacol Sci* **34**, 385–392.
- Zadeh AD, Xu H, Loewen ME, Noble GP, Steele DF & Fedida D (2008). Internalized Kv1.5 traffics via Rab-dependent pathways. *J Physiol* **586**, 4793–4813.
- Zeng G, Nystrom FH, Ravichandran L V, Cong LN, Kirby M, Mostowski H & Quon MJ (2000). Roles for insulin receptor, PI3-kinase, and Akt in insulin-signaling pathways related to production of nitric oxide in human vascular endothelial cells. *Circulation* **101**, 1539–1545.
- Zhang Y, Wang H, Wang J, Han H, Nattel S & Wang Z (2003). Normal function of HERG K⁺ channels expressed in HEK293 cells requires basal protein kinase B activity. *FEBS Lett* **534**, 125–132.
- Zhou Z, Gong Q, Epstein ML & January CT (1998a). HERG channel dysfunction in human long QT syndrome. Intracellular transport and functional defects. *J Biol Chem* **273**, 21061–21066.
- Zhou Z, Gong Q & January CT (1999). Correction of Defective Protein Trafficking of a Mutant HERG Potassium Channel in Human. *Biochemistry* **38**, 31123–31126.
- Zhou Z, Gong Q, Ye B, Fan Z, Makielski JC, Robertson G A & January CT (1998b). Properties of HERG channels stably expressed in HEK 293 cells studied at physiological temperature. *Biophys J* **74**, 230–241.